Journal of Huntington's Disease 2 (2013) 47–68
DOI 10.3233/JHD-130001
IOS Press

Research Report

A Transgenic Minipig Model of Huntington's Disease

Monika Baxa[a,b,1], Marian Hruska-Plochan[a,b,c,d,1], Stefan Juhas[a], Petr Vodicka[a,p], Antonin Pavlok[a], Jana Juhasova[a], Atsushi Miyanohara[e], Tetsuya Nejime[c], Jiri Klima[a], Monika Macakova[a,b], Silvia Marsala[c,d], Andreas Weiss[f,r], Svatava Kubickova[g], Petra Musilova[g], Radek Vrtel[h], Emily M. Sontag[i,j], Leslie M. Thompson[i,j,k], Jan Schier[l], Hana Hansikova[m], David S. Howland[n], Elena Cattaneo[o], Marian DiFiglia[p], Martin Marsala[c,d,q] and Jan Motlik[a,*]

[a]*Laboratory of Cell Regeneration and Plasticity, Institute of Animal Physiology and Genetics, v.v.i., AS CR, Libechov, Czech Republic*
[b]*Faculty of Science, Department of Cell Biology, Charles University in Prague, Prague, Czech Republic*
[c]*Neuroregeneration Laboratory, Department of Anesthesiology, University of California, San Diego, La Jolla, CA, USA*
[d]*Sanford Consortium for Regenerative Medicine, San Diego, La Jolla, CA, USA*
[e]*Vector Development Laboratory, Human Gene Therapy Program, Department of Pediatrics, University of California, San Diego, La Jolla, CA, USA*
[f]*Novartis Institutes for Biomedical Research, Neuroscience Discovery, Basel, Switzerland*
[g]*Department of Genetics and Reproduction, Veterinary Research Institute, Brno, Czech Republic*
[h]*Department of Clinical Genetics and Fetal Medicine, Palacky University, University Hospital Olomouc, Olomouc, Czech Republic*
[i]*Department of Biological Chemistry, University of California, Irvine, CA, USA*
[j]*Department of Psychiatry and Human Behavior, University of California, Irvine, CA, USA*
[k]*Department of Neurobiology and Behavior University of California, Irvine, CA, USA*
[l]*Institute of Information Theory and Automation v.v.i., AS CR, Prague, Czech Republic*
[m]*Laboratory for Study of Mitochondrial Disorders, First Faculty of Medicine, Department of Pediatrics and Adolescent Medicine, Charles University and General University Hospital in Prague, Prague, Czech Republic*
[n]*CHDI Foundation, Princeton, NY, USA*
[o]*Department of Pharmacological Sciences and Centre for Stem Cell Research, Università degli Studi di Milano, Milan, Italy*
[p]*Department of Neurology, Massachusetts General Hospital, Boston, MA, USA*
[q]*Institute of Neurobiology, Slovak Academy of Sciences, Kosice, Slovak Republic*
[r]*IRBM Promidis, Pomezia, Italy*

[1]The first two authors contributed equally to this work.

*Correspondence to: Jan Motlik, Institute of Animal Physiology and Genetics, v.v.i, Laboratory of Cell Regeneration and Plasticity, Rumburska 89, 27721 Libechov, Czech Republic. Tel: +420 315639560; Fax: +420 315639510; E-mail: motlik@iapg.cas.cz.

ISSN 1879-6397/13/$27.50

Abstract.

Background: Some promising treatments for Huntington's disease (HD) may require pre-clinical testing in large animals. Minipig is a suitable species because of its large gyrencephalic brain and long lifespan.

Objective: To generate HD transgenic (TgHD) minipigs encoding huntingtin (HTT)1–548 under the control of human HTT promoter.

Methods: Transgenesis was achieved by lentiviral infection of porcine embryos. PCR assessment of gene transfer, observations of behavior, and postmortem biochemical and immunohistochemical studies were conducted.

Results: One copy of the human HTT transgene encoding 124 glutamines integrated into chromosome 1 q24-q25 and successful germ line transmission occurred through successive generations (F0, F1, F2 and F3 generations). No developmental or gross motor deficits were noted up to 40 months of age. Mutant HTT mRNA and protein fragment were detected in brain and peripheral tissues. No aggregate formation in brain up to 16 months was seen by AGERA and filter retardation or by immunostaining. DARPP32 labeling in WT and TgHD minipig neostriatum was patchy. Analysis of 16 month old siblings showed reduced intensity of DARPP32 immunoreactivity in neostriatal TgHD neurons compared to those of WT. Compared to WT, TgHD boars by one year had reduced fertility and fewer spermatozoa per ejaculate. *In vitro* analysis revealed a significant decline in the number of WT minipig oocytes penetrated by TgHD spermatozoa.

Conclusions: The findings demonstrate successful establishment of a transgenic model of HD in minipig that should be valuable for testing long term safety of HD therapeutics. The emergence of HD-like phenotypes in the TgHD minipigs will require more study.

Keywords: Huntington's disease, mutant huntingtin, minipigs, large animal model, lentiviral transgenesis, FISH analysis, mRNA and protein expression, immunohistochemistry, DARPP32, AGERA assay, TR-FRET assay, spermatozoa

ABBREVIATIONS

AGERA	Agarose gel electrophoresis for resolving aggregates
HD	Huntington's disease
HTT	Huntingtin
TgHD	Transgenic HD
TR-FRET	Time-Resolved Förster Resonance Energy Transfer

INTRODUCTION

Huntington's disease (HD) is an inherited autosomal dominant neurodegenerative disorder with a worldwide prevalence of 3–10 affected individuals per 100,000 persons in Western Europe and North America [1, 2]. Progressive impairment of motor, emotional and cognitive functions [3, 4] is a consequence of the expansion of the CAG repeat stretch in exon 1 of the gene encoding huntingtin (HTT) protein [5]. The onset and the severity of HD correlates inversely with CAG repeat number [6]. The current pharmacotherapy of HD provides improvement of symptoms but no treatment is available to stop disease progression [7, 8].

Animal models are important tools to evaluate therapies for neurodegenerative disorders. Models of HD in rodent, Drosophila, C. elegans, and non-human primate have been generated. In general, each of these models shows some biochemical and neuronal features similar to HD in humans [2, 3]. Rodent and fly models of HD have been very useful for understanding the molecular basis for behavioral and neuronal abnormalities [2]. Although rodent models of HD that express either truncated [9–11] or full-length [12, 13] human mutant HTT display differences in onset and severity of phenotypes, these models collectively have provided valuable information related to target validation and drug therapy. However, the rodent's small brain size and differences in neuroarchitecture to humans limits their use for detailed neuroanatomic characterization associated with HD [14–17] and for adapting methods such as non-invasive imaging that are used in human clinics [18–20]. Large HD genetic models such as sheep [21] and the non-human primate [22] have been generated to help address these problems.

Pigs, and mainly minipigs, represent an optimal model for preclinical drug trials and long-term safety studies [20, 23–26]. This species has a physiology resembling in several aspects that of humans [27–29]. The large size of the pig brain permits detailed identification of brain structures by imaging techniques such as PET [30–32] and MRI [33–39]. There has been recent progress in defining the porcine genome [40–43], porcine single nucleotide polymorphisms [44], microRNAome [45–47], and improved techniques for genetic modification of pigs [48–51]. The porcine homologue of the huntingtin gene has a large ORF of 9417 nucleotides encoding 3139 amino acids with a predicted size of 345 kDa (GenBank, Accession No. AB016793). There is a 96% similarity between

the porcine and human huntingtin genes (GenBank, Accession No. AB016794). The number of CAG repeats in the porcine HTT gene is polymorphic, ranging from 8 to 14 units, and falls within the range of the normal human huntingtin gene [52]. Similar to humans, miniature pig possesses two HTT transcripts of approximately 11 and 13 kb [52, 53]. The similarities between porcine and human huntingtin genes and proteins have provided further impetus to use the pig as a model of HD [20, 54].

Recently, a cloning strategy was used to generate a transgenic HD minipig. Unfortunately, this porcine model suffered frequent perinatal mortality for reasons that are unclear [55]. Here we used a strategy based on lentiviral infection of porcine embryos and report the successful germ line transmission through successive generations (F0, F1, F2 and F3 generations) of a HD transgene encoding the first 548 aa of HTT with 124 glutamines under the control of human HTT promoter. Mutant protein expression is detected in both CNS and non-CNS tissues and in brain is comparable to the endogenous huntingtin. DARPP32 immunoreactivity in a 16 month old TgHD minipig was reduced compared to a WT sibling. At about one year of age, sperm number and oocyte penetration were severely affected in TgHD minipigs. These findings suggest that we have in hand a suitable large animal model for evaluating potential HD therapeutics.

MATHERIALS AND METHODS

Supplementary data

Supplementary Data (S1 –S8) are placed on the website of The Institute of Animal Physiology and Genetics, v.v.i.: www.iapg.cas.cz/CentrumPIGMOD/JHD

Minipigs

The Institute of Animal Physiology and Genetics in Libechov imported the first miniature pigs in 1967 from the Hormel Institute, University of Minnesota (two boars and three sows) and from the Institute for Animal Breeding and Genetics, University of Göttingen, Germany (two boars and four sows). Since then breeding, animal health and body shape have been thoroughly controlled and outbreeding conditions maintained by import of several additional boars from Göttingen [29]. Through continuous selection there has been an increase in the average litter size (now about 6–8 piglets) and maintenance of a white color, which has enabled the study of epidermal stem cells [56]. The animals were bred beginning at about 5 months of age when they reach sexual maturity. At this stage they weigh about 12–15 kg. In our minipig colony longevity is unknown because animals are housed for a maximum of about 8 years. However, the survival of parental minipig breeds (Hormel and Göttingen) has been reported to be 12 to 20 years. In this study, as is standard practice, the gilts (sexually mature, regularly estrous cycling minipig females) and weaned sows were housed in groups of 3–4 minipigs, and boars were kept individually. The regular estrous cycle (20 days) facilitated reproductive experiments.

All components of this study were carried out in accordance with the Institutional Animal Care and Use Committee of Institute of Animal Physiology and Genetics, v.v.i. and conducted according to current Czech regulations and guidelines for animal welfare and with approval by the State Veterinary Administration of the Czech Republic. The ample body size of the minipigs made feasible all surgical and laparoscopic approaches and their execution in a timely way. General anesthesia of minipigs was induced by TKX mixture (Tiletaminum 250 mg, Zolazepamum 250 mg, Ketamine 10% 3 ml, Xylazine 2% 3 ml) in a dose of 1 ml per 10 kg of body weight for experimental procedures including embryo transfer and oocyte collection. All surgery was conducted under sterile conditions in a standard surgical room. Postoperative care included treatment with analgesics and antibiotics. Animals were housed separately during recovery from anesthesia and then returned to the animal colony. Profound barbiturate anesthesia (Thiopental Valeant, 1g, i.v.) was used for transcardial perfusions.

Construction and production of the HIV1-HD-548aaHTT-145Q vector and verification of vectors in vitro

N-terminal truncated form of human huntingtin was created from the plasmid pFLmixQ145 comprising human full-length HTT cDNA with 145 CAG/CAA repeats (obtained from Coriell Cell Repositories, Camden, NJ). The first 548 aa of huntingtin (ending with residues AVPSDPAM) and including 145 Q was ligated with the HD promoter and inserted into the backbone plasmid pHIV7, which contained cPPT and WPRE cis-enhancing elements. Lentiviral vectors were produced by transient cotransfection of HEK293T cells. HIV1-CMV-EGFP vector (1×10^9 IU/ml) was used as the standard (See Supplementary Data S1 for details). Transgene expression was tested on porcine differentiated neural stem

cells. Subsequently, transduction potential of lentiviral vectors was evaluated using porcine zygotes. Matured porcine oocytes were laparoscopically aspirated from pre-ovulatory follicles. After IVF, embryos at pronuclear stage were microinjected with 10–20 pl of HIV1-CMV-EGFP construct into the perivitelline space and cultured into the blastocyst stage *in vitro* (See Supplementary Data S2 for details).

Transgenesis

Gilts were synchronized by Regumate (Jenssen Pharmaceuticals) (5 donors and 3 recipients per experiment). Donor females were superovulated by administration of pregnant mare's serum gonadotropin (PMSG) (Intervet International B.V.) and ovulation was induced by GnRH (Intervet International B.V.). After mating with the boars, pronuclear stage embryos were flushed from oviducts and microinjected into the perivitelline space with HIV1-HD-548aaHTT-145Q lentiviral vector (50–100 viral particles per zygote). The injected embryos were laparoscopically transferred into the fallopian tubes of recipients (See Supplementary Data S3 and S4 for details).

Genotyping

Biopsies of porcine skin were used to obtain DNA which was purified using DNeasy Blood & Tissue kit (Qiagen). The presence of the transgene was determined by PCR amplification of the region containing the WPRE coding sequence within the transgene (254 bp amplicon). Each PCR reaction contained 0.75 ng/μl of purified gDNA in 20 μl of reaction mixture and underwent 32 cycles of amplification (94°C for 30 s, 56°C for 40 s, 72°C for 40 s) following an initial 3 min denaturation period. SELK gene (360 bp amplicon) was used as an endogenous control. Primer sequences:

WPRE Fwd: 5′ GAGGAGTTGTGGCCCGTTG TCAGGCAACG 3′
WPRE Rev: 5′ AGGCGAGCAGCCAAGGAAA GGACGATG 3′
SELK Fwd: 5′ ACAGGCCCAAACTAATAAGAG 3′
SELK Rev: 5′ CAAATTTGGAGCCTTTTGT 3′

Fluorescent in situ hybridization

The localization of transgenes within the porcine genome was detected by Fluorescence *in situ* hybridization (FISH) analysis [57]. Mutant HTT sequence from the recombinant plasmid (HIV1-HD-548aaHTT-145Q) was labeled with biotin-16-dUTP (Roche Diagnostics GmbH) using a nick transcription kit (Abbott). The resulting probe did not detect the endogenous porcine HTT gene. Immunodetection and amplification were performed using avidin-FITC and anti-avidin-biotin. Chromosomes were counterstained with propidium iodide and DAPI. Karyotyping was determined using image analysis of reverse DAPI banding.

Microdissection of chromosomes and analysis of copy number variation

The incorporation of transgenic HTT into the q arm of chromosome 1 was confirmed by microdissection of q arms of both chromosomes 1 followed with a non-specific degenerate oligonucleotide-primed (DOP) PCR. 2 μl of DOP PCR amplification product were used as a template to carry out PCR amplification of the transgene.

Primer sequences:

MDS Fwd: 5′ TTCATAGCGAACCTGAAGTC 3′
MDS Rev: 5′ TTGTGTCCTTGACCTGCTGC 3′

The number of copies of the transgenes integrated into the porcine genome was determined using relative comparison of quantitative DNA amplification between the endogenous porcine HTT and the transgenic human HTT. HTT primers and probe 6-carboxyfluorescein, (6-FAM, TaqMan Probe, Applied Biosystems) were designed to detect HTT of both species. ACTB (VIC, TaqMan Probe, Applied Biosystems) was used as a reference gene. Each multiplex qPCR reaction was performed in a reaction volume of 20 μl using TaqMan Gene Expression chemistry (ROX passive reference, Applied Biosystems) using 75 cycles of amplification (30 s at 94°C, 30 s at 51.1°C, 30 s at 72°C) following an initial 3 min denaturation period. The qPCR data were analyzed using LinRegPCR software [58].

The sequences of the oligonucleotides:

HTT TaqMan MGB Probe: 6-FAM-TCTGCGTC ATCACTGC-MGBNFQ
HTT Primer Fwd: 5′ CTTCTGGGCATCGCTATG 3′
HTT Primer Rev: 5′ CATTCGTCAGCCACCATC 3′
ACTB TaqMan MGB Probe: VIC-AGTCCCTG CCTTCCCAAA-MGBNFQ

ACTB Primer Fwd: 5′ GTCATTCCAAGTATCAT GAGATG 3′
ACTB Primer Rev: 5′ TGGAGTACATAATTTA CACTAAAGC 3′

Determination of glutamine number in human mutant huntingtin

The number of glutamines in human mutant HTT was determined by PCR using primer pairs that flanked the region of the CAG/CAA repeat. The length of the PCR fluorescently labeled product was detected using Fragment analysis on an Applied Biosystems 3130 Genetic Analyzer. Samples were separated in gel polymer POP-7 gel at 60°C using LIZ 600 size standard. Data analysis was performed by GeneMapper® software.

Primer sequences:

HD1: 5′ ATGAAGGCCTTCGAGTCCCTCAAGT CCTTC 3′ (6-FAM)
HD3pig: 5′ CGGCGGCGGTGGCGGTTGCTGT TGCTGCTG 3′

PCR protocol: 95°C for 5 min, followed by 40 cycles of denaturation at 94°C for 30 s, annealing at 70°C for 30 s and elongation at 72°C for 30 s with a final extension of 3 min.

Detection of mRNA expression of mutant human HTT

Purified RNA was obtained from cultured porcine skin fibroblasts using RNeasy Plus minikit (Qiagen). RT PCR amplification was performed in a reaction mixture containing 2.0 ng/μl of total RNA with reaction volume of 20 μl. The primer set for RNA huntingtin insert (1446 bp amplicon) was designed using Beacon Designer. ACTB (∼100 bp amplicon, PrimerDesign Ltd) was used as a reference gene. The HTT amplification was performed in one step starting with reverse transcription at 50°C for 30 min and denaturation at 95°C for 15 min, followed by 50 cycles of denaturation at 94°C for 45 s, annealing at 56°C for 45 s and elongation at 72°C for 95 s with the final extension of 2 min. The amplification of ACTB reference gene was performed in a one-step reaction (50°C for 30 min, 95°C for 15 min, followed by 35 cycles of amplification at 94°C for 45 s, 61°C for 30 s and 72°C for 30 s with the final extension of 3 min. Reaction mixtures missing reverse transcriptase were included for each animal sample to exclude the possibility of contamination with genomic DNA.

Primer sequences:

HTT RNA Fwd: 5′ GAAACTTCTGGGCATCGC TATG 3′
HTT RNA Rev: 5′ GAAAGCCATACGGGAAG CAATAG 3′

Biochemical assays

Eight minipigs at the age of 4 ($N = 4$), 10 ($N = 2$) and 16 months ($N = 2$) from F2 generation (4 TgHD + 4 WT) were perfused under deep anesthesia with ice-cold PBS. The left hemisphere of each perfused brain was dissected and used in biochemical assays (SDS-PAGE and Western blot and TR-FRET). Brain and tissue biopsies were stored at –80°C.

15 μg of total protein from crude homogenates of TgHD minipig and WT littermates samples were diluted by NuPage 4× LDS sample buffer (LifeTech #NP0007) and 0.1 M DTT. Samples were loaded onto 3–8% Tris-acetate (LifeTech #EA03755) gel and run at 125 V in Tris-Acetate SDS Running Buffer (LifeTech #LA0041) until the 30 kDa band of Novex Sharp protein standard (LifeTech #LC5800) had migrated to the end of the gel. Gels were then immersed in transfer buffer containing 1% SDS and 20% MetOH for 8 minutes and then transferred onto nitrocellulose membrane (LifeTech #IB301001) using an iBlot gel transfer device (LifeTech #IB1001) P3 for 8 minutes. Membranes were blocked with 5% milk for 30 min at RT (BioRad #170-6404) and probed with anti-HTT antibody (Ab1, 1:1,000; [59]) overnight at 4°C. Membranes were then incubated for 1 h at RT in a 1:5,000 dilution of Peroxidase-conjugated Donkey Anti-Rabbit secondary antibody (Jackson ImmunoResearch #711-035-152); followed by 5 min incubation in Supersignal West Pico (Pierce #3408). Signal was detected on autoradiographic film (GE Healthcare #28906839). Membranes were stripped by Re-Blot Plus Strong Solution (10×) (Millipore #92590) for 15 minutes at RT, blocked by 5% milk and re-probed with anti-actin antibody in a 1:500 dilution (Sigma #A4700). After 1 h incubation at RT in secondary Donkey anti-Mouse antibody (Jackson ImmunoResearch #715-0350150), detection was performed as described above.

SDS-agarose gel electrophoresis for resolving aggregates (AGERA) and Western blot analysis

The analysis of mutant HTT oligomers by SDS-AGE and Western analysis was performed as described previously [60–63]. 50 μg of total protein from

crude homogenates of TgHD minipig samples were diluted 1:1 into non-reducing Laemmli sample buffer (150 mmol/l Tris-HCl pH 6.8, 33% glycerol, 1.2% SDS and bromophenol blue). Purified ferritin (440 kDa) was used as a high molecular weight size marker and positive indicator of migration and transfer of protein (Sigma). Eight week old R6/2 mouse striatal tissue was used as a positive control for mutant HTT oligomers [63]. Samples were loaded onto 1% agarose gel containing 0.1% SDS and run at 100 V in running buffer (192 mM glycine, 25 mM Tris-base, 0.1% SDS) until the bromophenol blue dye front had migrated 12 cm. The gel was transferred onto PDVF membrane (Millipore) at 200 mA for 1 h in transfer buffer (192 mM glycine, 25 mM Tris-base, 0.1% SDS, 15% MetOH) using Semi-dry electroblotter model HEP-1 (OWL Scientific). The thickness of the 1% gels decreased substantially during transfer, so the electroblotter was tightened periodically to ensure constant and even contact between the gel sandwich and the electroblotter. After transfer, the membrane was blocked for 1 h in StartingBlock™ T20 (TBS) Blocking Buffer (Pierce) at room temperature and incubated in a 1:500 dilution of anti-HTT antibody (Millipore MAB5374, EM48) overnight at 4°C. The membrane was then incubated for 1 h in a 1:10,000 dilution of Horseradish peroxidase-conjugated anti-mouse secondary (Jackson ImmunoResearch Laboratories) at room temperature and signal was detected using Supersignal West Pico (Pierce).

Filter retardation assay

The same homogenates used in the AGERA assays were also analyzed for SDS-insoluble mutant HTT by filter-retardation assay as previously described [62–64]. 50 μg of homogenate were diluted in 0.1% SDS and filtered through cellulose acetate membrane (Schleicher & Schuell, 0.2 μm pore size) using a dot blot filtration apparatus (Bio-Rad) and washed using 0.1% SDS. The blot was then blocked for 1 h in 5% non-fat milk at room temperature and probed with primary and secondary antibodies and developed as described above.

TR-FRET quantitative analysis

TR-FRET (Time-Resolved Förster Resonance Energy Transfer) quantification of soluble mutant huntingtin was performed as previously described [65]. In short, 5 μl tissue sample homogenates and 1 μl detection buffer (50 mM NaH_2PO_4, 400 mM NaF, 0.1% BSA and 0.05% Tween + detection reagents) were added per well of a low-volume 384-well plate. The labeled antibodies used for detection of soluble mutant HTT were 2B7 bound to terbium cryptate (TB) and MW1 bound to D2 fluorochrome. The final amounts of antibodies were 1 ng 2B7-Tb and 10 ng MW1-D2. After incubation for 1 h at room temperature, samples were analyzed by excitation of the Terbium donor at 320 nm. After a time-delay of 100 μs, TB and D2 emission signals were detected at 620 and 665 nm with an Envision reader (PerkinElmer, Switzerland). TR-FRET signals are presented as the total protein normalized ratio of 665 nm signal divided by 620 nm signal. This calculation benefits from the internal signal intensity reference of the TB donor fluorescence, thereby providing a mutant HTT protein signal corrected for potential assay-interfering artifacts such as turbidity, light scattering or quenching capability of the sample, differences in sample volume due to slight pipetting variability, and day-to-day assay fluctuation caused by differences in excitation lamp energy.

Immunohistochemistry

The right hemisphere of each perfused brain was immersed in a fixative solution composed of 4% paraformaldehyde (PFA) in phosphate buffer saline (PBS, pH 7.4) for 5–6 days and then embedded in HistOmere [66, 67] for 2–4 minutes in dorso-ventral direction, so that the optic chiasm and mammillary bodies were in horizontal position, and cut into 6 slabs. Brain slab no. 2 contained the majority of the neostriatum. The brain slabs were post-fixed in 4% PFA for another 7–10 days and then placed into 30% sucrose containing 0.01% sodium azide. 40 μm thick coronal brain sections were cut using a clinical cryostat (Leica Biosystems, CM1950). The endogenous peroxidase activity was blocked with a solution of 0.3% of hydrogen peroxide in MetOH for 20 min and the free-floating sections were immunostained using the following primary antibodies listed with dilutions and sources: Ab1 (1:1,000, [59]), AB585 (1:500, [59]), MW8 (supernatant, Hybridoma Bank, University of Iowa, USA), mEM48 (1:50, MAB5374, Millipore) and DARPP32 (1:15,000, ab40801, Abcam). Secondary goat fluorescent antibodies (Alexa Fluor® 488, Alexa Fluor® 555, Alexa Fluor® 647 from Invitrogen, Life Technologies) were used for visualization of some primary antibodies. Some sections were treated with biotinylated secondary antibodies (1:400, Amersham, Buckinghamshire, UK) followed by avidin-peroxidase complex (1:400, A3151; Sigma-Aldrich). The avidin-peroxidase complex was visualized by incubation with DAB tablet (#4170, Kementec Diagnostics). The sec-

tions were finally mounted with DePeX (Sigma). Analysis was performed using a confocal microscope equipped with 4 lasers (405, Argon, 561 and 633 nm lasers) (SP5, Leica Microsystems), virtual microscopy scanners (VS110®-5, Olympus, NanoZoomer 2.0-HT, Hamamatsu) and a light microscope (Primo Star, Zeiss).

Determination of the number and intensity of DARPP32 + neurons

Images of regions of caudate and putamen were obtained using the confocal microscope and a HCX PL APO lambda blue 63.0 × 1.40 OIL UV objective to detect DAPI staining. PMT setup, pinhole sizes (1 Airy) and contrast values were kept constant across different sessions. The number of coronal sections analyzed per caudate nucleus and putamen ranged from 3–5 and 25 areas were scanned in each section. Areas of analysis were sectioned in the *z plane* in 1-micron optical sections (13–20 μm) using FiJi software (http://fiji.sc) and only cells confirmed to include the entire DAPI stained nucleus were included in the analysis. This sampling method is an optical dissector technique and minimizes sampling errors (due to partial cells) and stereological concerns, as minor variations in cell volumes do not influence sampling frequencies [68, 69]. The DAPI staining in DARPP32 labeled cells revealed nuclei of two distinct morphologies-large grainy nuclei mainly in the caudate nucleus and smaller compact nuclei mainly in putamen. Only cells with DARPP32 labeling and these nuclear features were included in the analysis. A total of 5,256 neurons in TgHD minipig and 3,644 neurons in WT minipig were counted. All values were reported as the number of neurons positive for immunoreactive DARPP32 per mm^3 tissue. In the same scanned areas used for the cell based analysis the overall intensity of DARPP32 signal was also measured. The average signal intensity was determined for all images in a stack and expressed as the mean intensity.

Semen collection and penetration test

Semen samples from 2 transgenic boars of F1 generation (G117 and G118) and 3 wild type boars (F808, F630, F719) were collected starting at age 12 months and periodically over 14 months. Five and 18 samples were taken for the WT and 16 and 18 for the TgHD minipigs. Total number of spermatozoa per ejaculate was estimated by Sperm Class Analyzer (Microptic, Spain). Differences in the number of spermatozoa between individual boars were analyzed using Kruskal-Wallis test followed by Mann-Whitney U test for the *post hoc* comparison. Values of $p < 0.05$ were considered significant. The spermatozoa were prepared for *in vitro* penetration test by double centrifugation (20 min/600 g, 10 min/600 g) and the following swim-up procedure [70] provided about 1×10^6 cells for *in vitro* fertilization. The cycling minipig gilts were synchronized by Regumate (Jenssen Pharmaceuticals) and superovulated by administration of PMSG (Intervet International B.V.). Ovulation was inducted by GnRH (Intervet International B.V.). The oocyte-cumulus complexes were isolated from large antral follicles 72 h after PMSG injection at the germinal vesicle stage and they were cultured for 40–44 h up to metaphase II with the first polar body [70]. In 13 independent experiments, oocytes with intact zona pellucida were used. In some experiments, the zona pellucida was removed by incubation with 0.25% pronase. After 24 h of incubation with spermatozoa, oocytes were mounted on slides, fixed in acetic-alcohol, stained with acetic-orcein and examined with phase contrast microscopy. The penetration rate into matured pig oocytes was recorded. Differences among individuals in penetration rate were analyzed using Kruskal-Wallis test followed by Mann-Whitney U test used for the *post hoc* comparison between individual boars and values of $p < 0.05$ were considered significant.

RESULTS

Generation and characterization of TgHD minipig

The HIV1 backbone plasmid pHIV7, which contains cPPT and WPRE cis-enhancing elements (Supplementary Data S1), was used for the construction of a lentiviral vector carrying the sequence of the first 548 amino acids of human HTT protein containing 145 glutamines under the control of human HD promoter (Fig. 1A). The transduction potential of the lentiviral construct was verified on porcine zygotes using the HIV1-CMV-EGFP construct. Efficient transduction of porcine embryos was confirmed by the presence of EGFP fluorescence in embryoblasts and trophoblasts (Supplementary Data S2).

The TgHD minipigs were generated by using microinjection of HIV1-HD-548aaHTT-145Q construct into the perivitelline space of the one-cell stage porcine embryos (Supplementary Data S3). Twenty-nine injected zygotes were transferred to recipient sows via laparoscopy (Supplementary Data S4). After standard duration of gravidity (115 days), the first

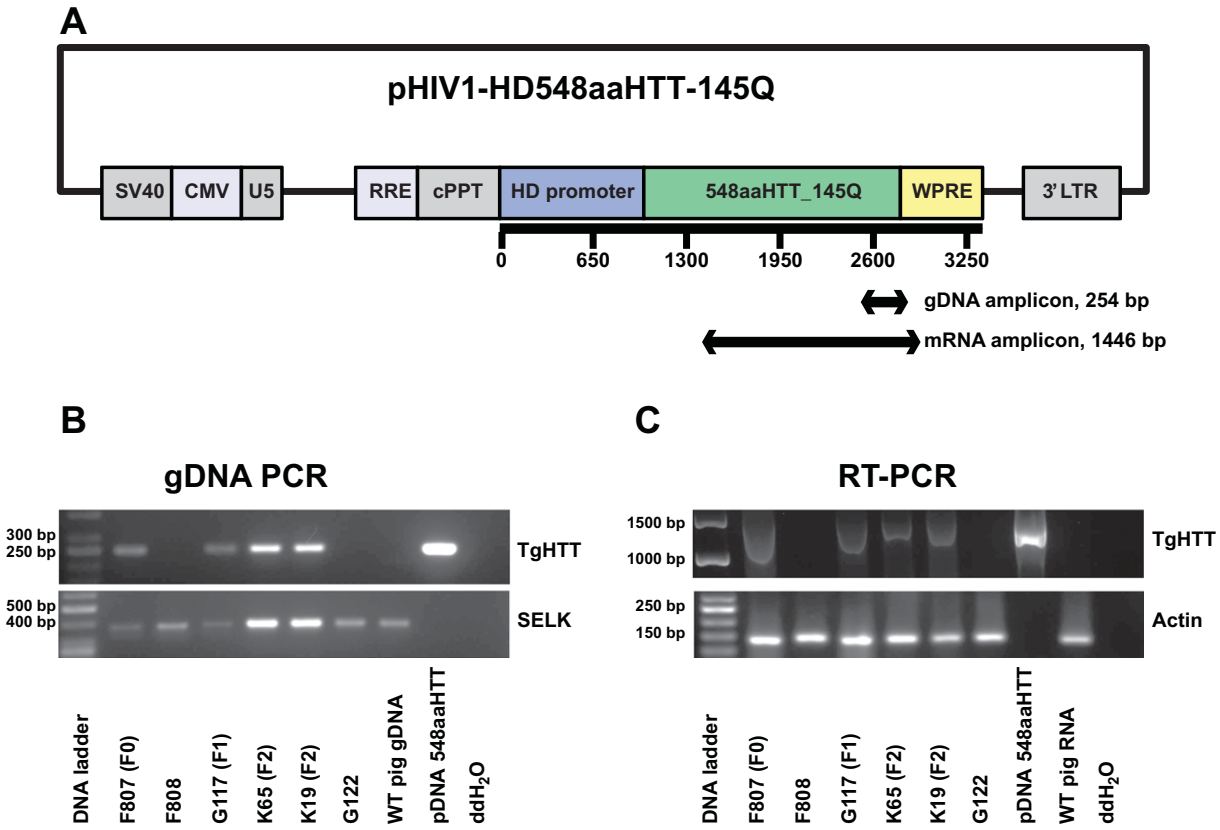

Fig. 1. Molecular characterization of TgHD minipigs. (A) Schematic of the first 548aa of human HTT cDNA fragment with the stretch of 145 glutamines ligated to human HTT promoter in the pHIV7 backbone. WPRE primer set (gDNA amplicon) was used for genotyping the animals. 548aaHTT primer set (mRNA amplicon) was used for confirmation of mRNA expression. (B) PCR of the human HTT and WPRE region (TgHTT) shows presence of transgene in porcine DNA. Amplification of SELK gene (360 bp amplicon) was used as control for the quality of DNA. (C) Expression of mRNA by RT PCR amplification of 1446 bp long amplicon spanning the region encoding human HTT and WPRE region. Amplification of actin mRNA (ACTB) was used as a control for RNA quality. Reaction mixtures without reverse transcriptase were included for each animal sample to exclude the possibility of genomic contamination (data not shown). Plasmid DNA with 548aaHTT-145Q construct was used as a positive control. WT pig genomic DNA and mRNA and ddH_2O were used as negative controls. Generation (F0, F1, F2) is indicated just for TgHD animals.

HIV1-HD-548aaHTT-145Q manipulated piglets were born. One gilt (F807) in a litter of 6 live newborns was transgenic. Two non-transgenic piglets died within 48 hours after birth (Fig. 2). The number of transgenic animals when expressed as a proportion of the number of live births or as a proportion of microinjected zygotes was 16.7% or 3.5%, respectively.

The F0 transgenic gilt was mated with its non-transgenic littermate to produce F1 generation. In the two litters of 17 newborns, five piglets were transgenic (Fig. 2). Germ line transmission to the F1 generation was 29.4%. F1 transgenic boars were sexually mature at the expected age of five months and they successfully produced offspring.

Of 92 F2 piglets born from seventeen litters – 73 survived (20.7% perinatal mortality) and 37 of these were transgenic (TgHD, black symbols, Supplementary Data S5) resulting in a 40.2% F2 generation transgenesis rate per born piglet. The number of piglets in a litter and newborn mortality was comparable between offspring of TgHD and WT animals (Supplementary Data S6). The proportion of TgHD and WT piglets in F2 generation were comparable, enabling creation of optimal experimental groups (TgHD vs. WT animals).

Five transgenic boars and one TgHD female of the F2 generation were bred and a total of 51 live WT and 30 live TgHD piglets were obtained from 23 litters. The incidence of perinatal mortality in F3 generation was 14.2% and the rate of transgenesis was 34.9%.

The F0 transgenic sow was also mated with an F1 transgenic boar. Four transgenic piglets were born in two litters (Supplementary Data S5). No homozygote TgHD transgenic offspring were obtained.

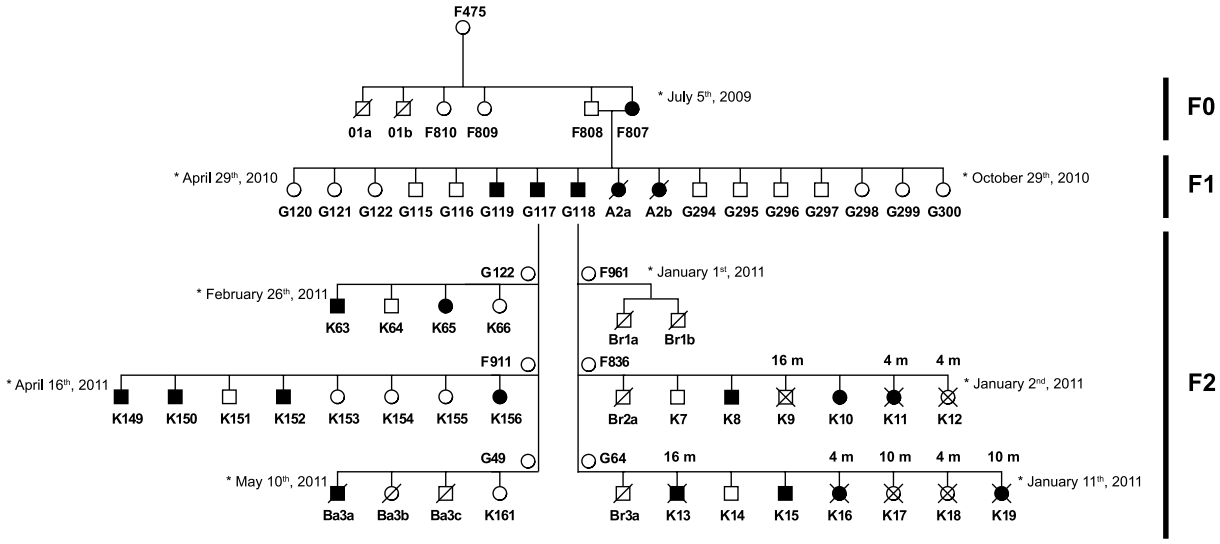

Fig. 2. Breeding and pedigrees of TgHD minipigs. Black boxes (males) and black circles (females) represent animals positively tested for the transgene in DNA extracted from biopsy of ear tissue. "/" denotes a dead minipig within the first 48 hours; "X" indicates an animal sacrificed for biochemical and microscopic studies. The F0 minipig gave birth to 5 TgHD piglets in two litters. Mendelian inheritance is indicated in the F2 generation.

DNA and RNA analysis

Genotyping was performed using PCR as described in Methods. Figure 1B demonstrates TgHD minipigs in F0, F1 and F2 generations. Expression of mRNA was confirmed by RT PCR amplification of the region encoding human HTT and WPRE region (Fig. 1C). To confirm mRNA expression of the full insert, primers were designed for amplification of the 1446 bp product from the 548aa HTT transgene. mRNA of mutant huntingtin was transcribed in all TgHD minipigs. Mutant HTT gene was detected by FISH analysis on chromosome 1 (1q24-q25) in animals from the first three generations (Fig. 3A). Microdissection of q arms of chromosomes 1 followed with non-specific DOP PCR confirmed the presence of the transgene in chromosome 1. Chromosomes 6 and 13 were used as negative controls (Fig. 3B).

Quantitative PCR was used to detect the presence of both endogenous wild type HTT gene and the mutant HTT transgene in the porcine genome. Assuming the presence of the two endogenous porcine HTT alleles, all the transgenic animals integrated 1 copy of the transgene in their genome (Fig. 3C). Furthermore, fragment analysis of the PCR amplicons of the DNA fragment containing CAG/CAA sequence showed that the integrated transgene was in frame and consisted of 124 CAG/CAA instead of the original 145 (Fig. 3D).

Development and behavior of TgHD minipigs

The development and behavior of the TgHD minipigs from F0, F1, F2 and F3 generations appeared comparable to WT. TgHD piglets looked normal at birth, were able to stand within a few minutes and their size was similar to each other and to WT. Social dominance relationships among the WT and HD littermates began forming two days after birth and as expected, changed as a consequence of weaning and sexual maturity. TgHD and WT animals of both sexes became sexually mature at the expected age of 5 months and were able to produce offspring. We noticed a decline in the fertility of the F1 generation TgHD boars beginning at about 12 months (see below). Motor deficits characteristic of HD were not evident in the TgHD animals. Lateral eye movements were smooth and vertical gaze movement was similar to WT minipigs. Saccades were not slow, facial praxis was normal, and vocalization had a normal rhythm. No involuntary movements were observed. A qualitative rating scale was developed to evaluate stance, gait, and ability to cross a barrier in TgHD and WT animals starting at age 3 months and at monthly intervals up to 30 and 40 months of age. A rating of 0 was normal and 3 was the most impaired (see Supplementary Data S7 for details). Using this rating scale, there was no difference in score for standing, gait, or crossing a barrier between WT (score = 0) and F0 TgHD minipigs (F807) up to 40 months and F1

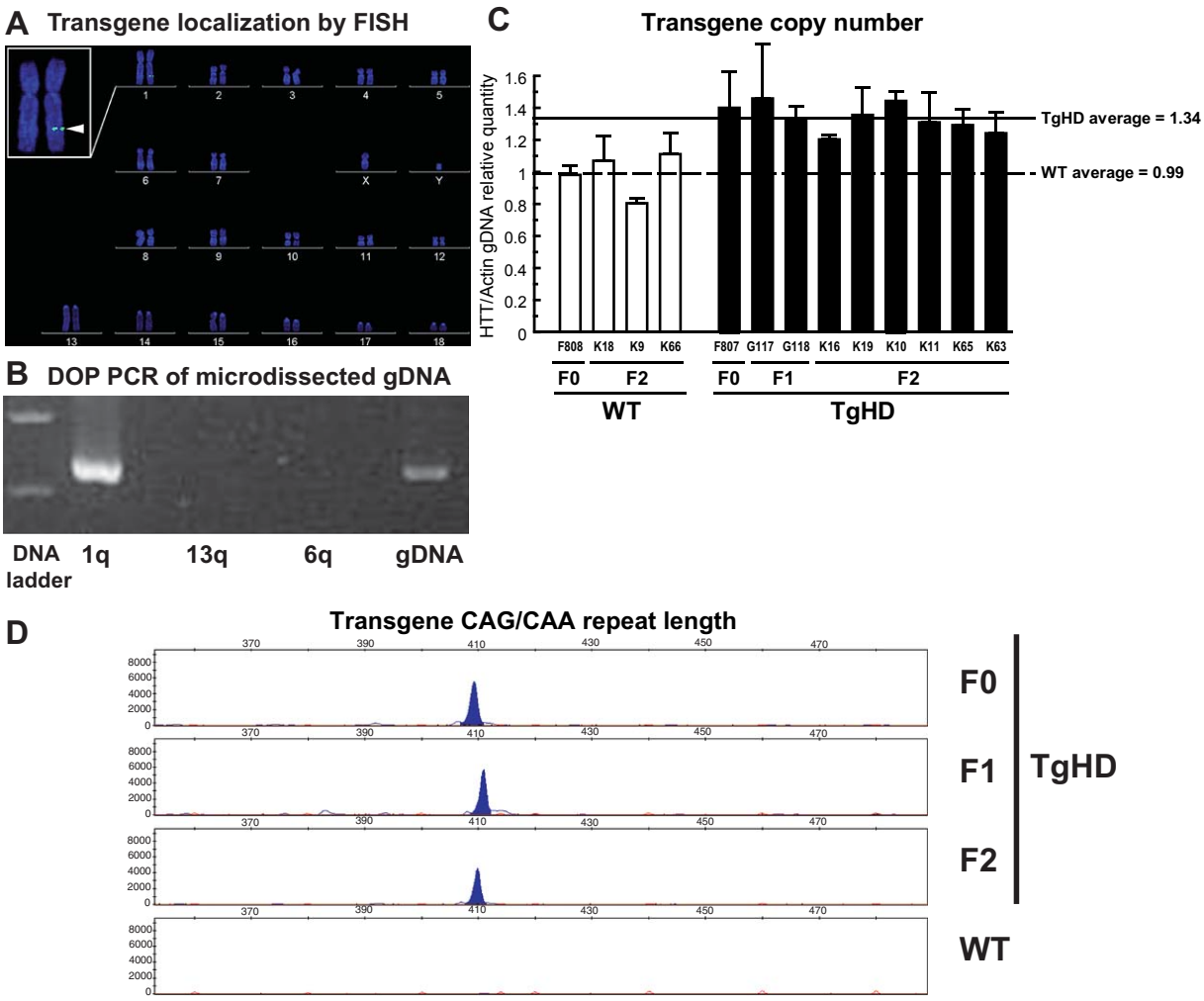

Fig. 3. Localization and copy number of mutant HTT and length of CAG/CAA repeat in TgHD minipig. (A) Incorporation of mutant HTT into the porcine genome. FISH technique shows the localization of the transgene on chromosome 1 (1q24-q25) (inset, arrowhead) of F1 TgHD male. (B) Microdissection of q arms of chromosome 1 followed by non-specific degenerate oligonucleotide primed (DOP) PCR confirms the presence of the transgene on chromosome 1 but not chromosomes 6 and 13. Genomic DNA from TgHD minipig was used as a positive control. (C) Bar graph shows quantity of HTT gDNA (both endogenous porcine HTT and human HTT transgene) in WT and TgHD animals relative to endogenous actin gDNA. Lines indicate mean values for the WT (dashed line) and transgenic animals (full line). Copy number of the transgene was determined by comparing its mean value to that of the WT. (D) The result of analysis of fragment length electrophoresis is shown. PCR amplification with primers specific for transgene shows a peak of 410 bp in TgHD animals but not in the WT. 410 bp fragment encodes both primer sequence and CAG/CAA repeat sequence encoding 124 glutamines in all three generations. CAG/CAA repeat number was similar in different porcine tissues (data not shown).

generation minipigs (G117, G118, and G122) up to 30 months of age (Scores = 0).

Expression of mutant huntingtin protein

Brain lysates were obtained from two 4 month old F2 TgHD minipigs and two WT minipigs. SDS-PAGE and Western blot analysis was performed as described in methods using antibody Ab1 to detect HTT. Mutant HTT protein fragment was detected in all regions of the CNS examined including motor cortex, putamen, caudate nucleus, hippocampus, hypothalamus, thalamus, cerebellum, and spinal cord (Fig. 4A top for one WT and one TgHD). Mutant HTT fragment migrated at the expected size of 120 kDa. Peripheral tissues including small intestine, lung, liver, kidney, ovaries and skin also expressed the TgHD protein whereas little or no transgenic HTT was present in stomach, heart, skeletal muscle and spleen (Fig. 4A bottom). With some exceptions (for example, hypothalamus), the densitometry

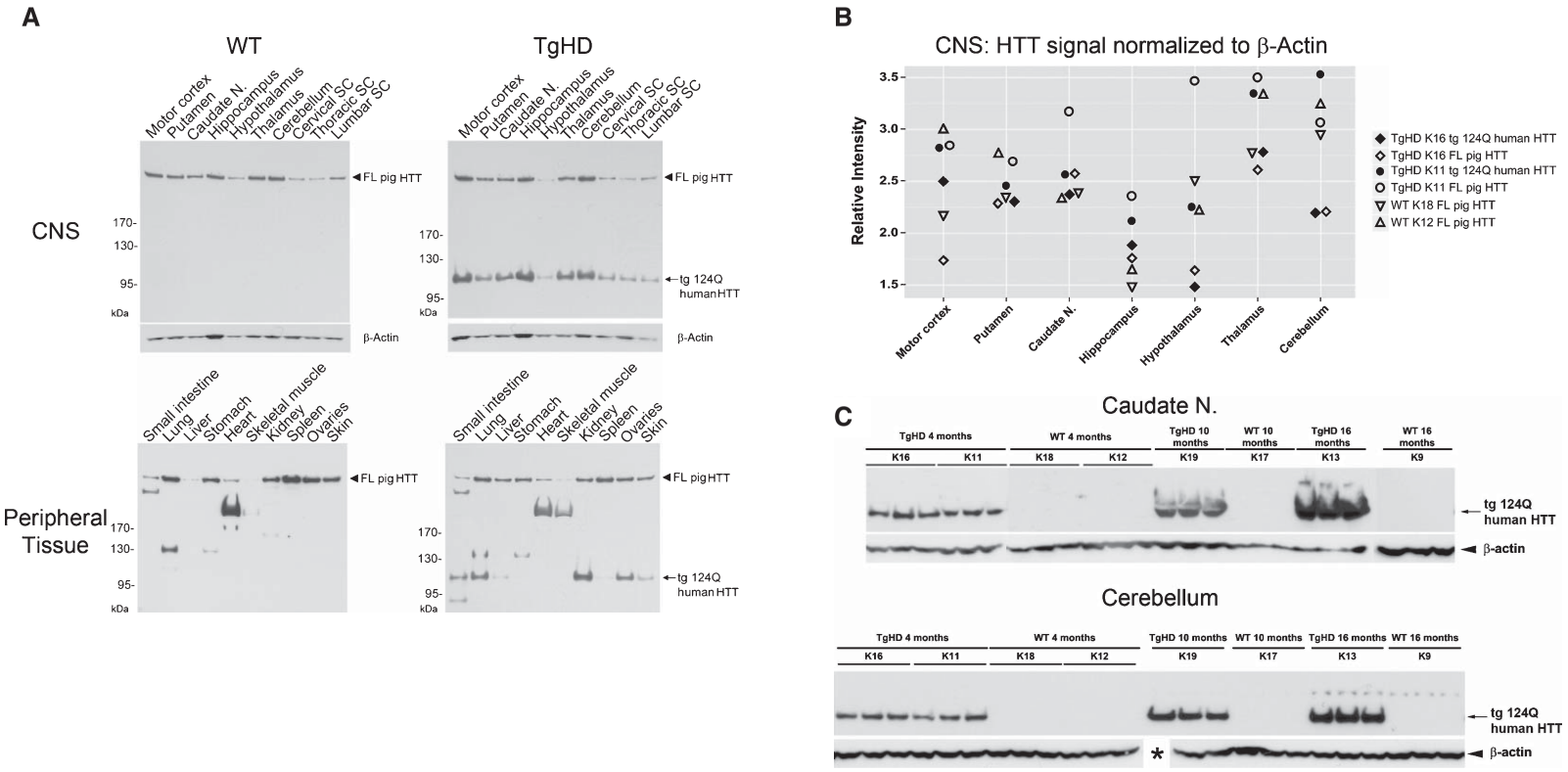

Fig. 4. Western blot analysis of mutant HTT protein in F2 WT and TgHD minipig. (A) Western blot immunoprobed with the anti-HTT1-17 antibody Ab1 shows expression of the porcine WT (FL-HTT and human HTT transgenic protein fragment (tg 124 Q human HTT) in different CNS and peripheral tissues of 4 month old minipigs. (B) Scatterplot of signal intensity values for pig huntingtin and mutant HTT relative to beta actin levels in different brain regions for WT and TgHD minipigs. (C) Western blot analysis of caudate nucleus and cerebellum from F2 – 4, 10 and 16 month old WT and TgHD minipigs. Samples of each animal are shown in triplicate. Actin is shown as loading control. Asterisk denotes missing actin band for one of triplicates of K19 cerebellum sample.

analysis showed that the levels of mutant HTT fragment in different brain regions were comparable to the levels of the endogenous porcine huntingtin seen on the same blots (see scatterplot, Fig. 4B). Further Western blot analysis of caudate nucleus and cerebellum was performed in frozen samples of brain from 8 minipigs (4 TgHD and 4 WT) ages 4, 10 and 16 months. Results showed that the mutant protein fragment was detected in the TgHD minipigs at all ages. The signals for the mutant protein migrated more broadly in SDS-PAGE in the caudate and cerebellum of the 10 and 16 months old minipigs than in the samples from the 4 month old minipig (Fig. 4C). Whether this characteristic of migration is related to an altered property of mutant HTT is unclear.

We quantified the levels of soluble mutant HTT in CNS and peripheral tissues of two sibling pairs of TgHD and WT minipigs using TR-FRET as described in Methods. Results in all brain and spinal cord regions and some peripheral tissues (lung, spleen, kidney, ovaries) showed robust HTT signal in TgHD animals compared to WT minipigs suggesting the assay was detecting mutant HTT (Fig. 5). To determine the presence of aggregated mutant HTT in TgHD minipig brain, AGERA and filter retardation assays were applied. Homogenates from motor cortex, putamen, caudate nucleus and cerebellum of WT and TgHD 16 month old minipigs were tested with mEM48 antibody. Based on these assays, aggregated mutant HTT was not present in the brain of TgHD minipig but was detected as expected in the brain of the R6/2 HD mouse (Fig. 6).

Immunohistochemistry of WT and TgHD brains

HTT immunoreactivity was examined by the immunoperoxidase method in the 4 month old minipig brain at the levels of the neostriatum using anti-HTT antibody Ab1 which detects HTT1–17. The cortex, caudate nucleus and putamen showed HTT immunoreactivity. Within these regions the gray matter was more strongly labeled than the white matter (Fig. 7). Consistent with findings in mice and human brain [71], endogenous HTT in WT minipig strongly localized to somatodendritic regions of cortical neurons and to cell bodies of neostriatal neurons. Neuropil of cortex and neostriatum was also strongly labeled. The other anti-HTT antibody which detected endogenous huntingtin in WT minipig was AB585, which was made to HTT585–725 [59]. There was no difference in the intensity of staining for HTT in TgHD minipig compared to WT minipig with anti-HTT Ab1. No nuclear inclusions were detected in the TgHD brain even though Ab1 antibody detects nuclear inclusions in the human HD cortex [72]. Antibodies MW8 and mEM48 are known to detect nuclear aggregates in other HD animal models but did not produce any staining in the TgHD minipig. Similarly no labeling was detected with MW8 in the 16 month old TgHD pigs.

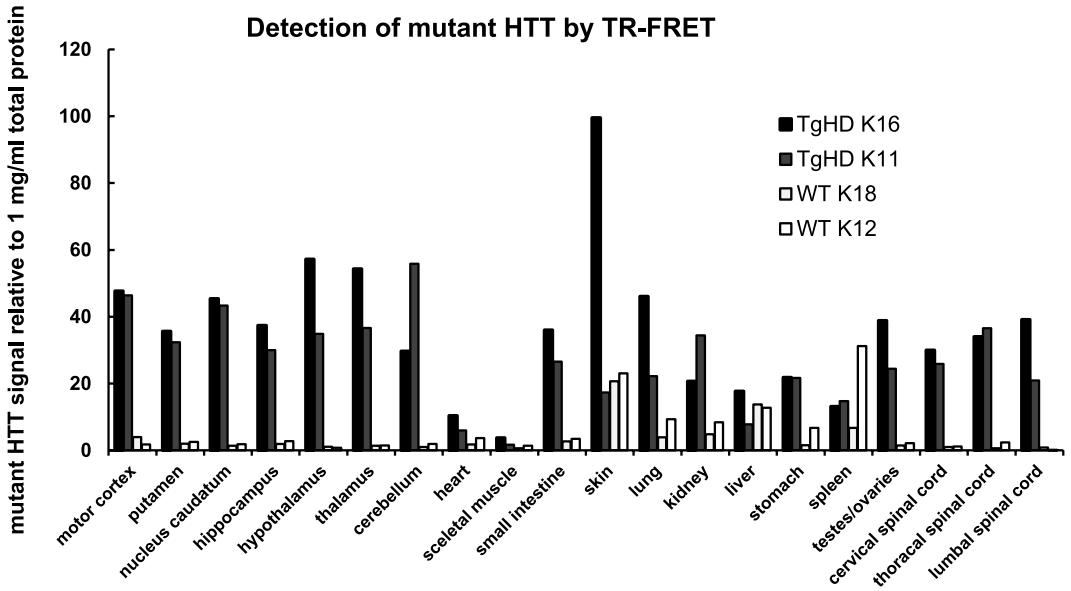

Fig. 5. TR-FRET analysis of soluble HTT protein in F2 WT and TgHD minipig. Bar graph shows results of TR-FRET analysis of soluble mutant HTT protein in TgHD and WT tissue samples (isolated from 4 month old minipigs) expressed as mutant HTT signal per 1 mg/ml total protein. Results of TR-FRET quantitative analysis correlated with western blot analysis shown in Fig. 4B.

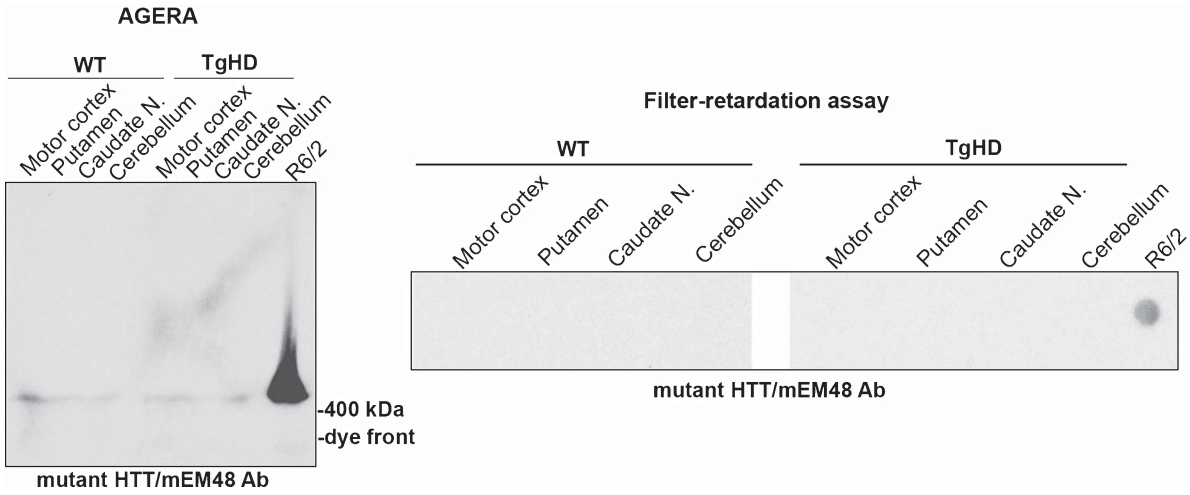

Fig. 6. Biochemical assays for detection of aggregated mutant HTT. AGERA and Filter retardation assays were performed as described in Methods using tissue from different brain regions of WT and TgHD minipig and R6/2 HD mouse. Membranes were probed with mEM48 antibody. Only R6/2 sample shows signal in both assays.

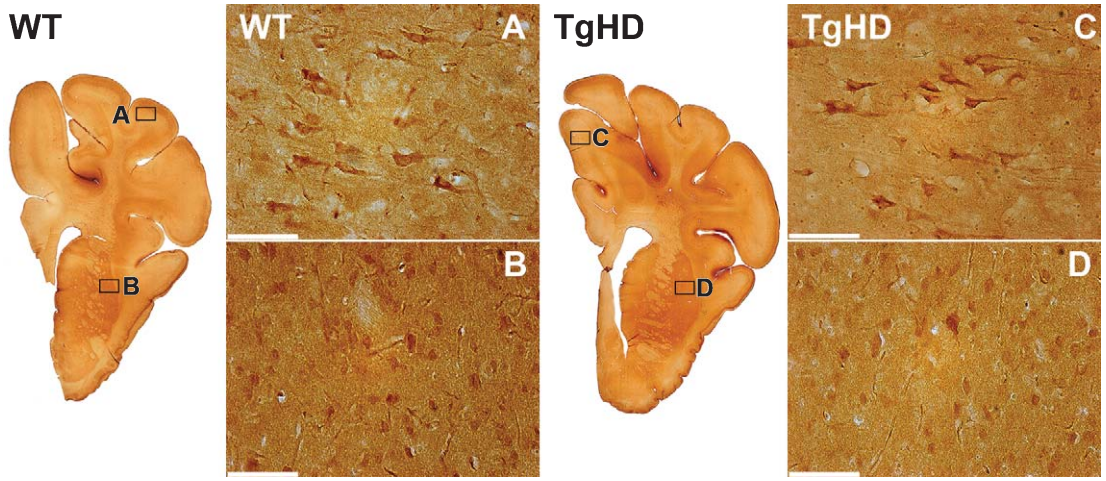

Fig. 7. HTT localization in the brain of WT and TgHD minipig. Shown are coronal sections of 4 month old WT minipig brain on the left and TgHD minipig brain on the right labeled using the immunoperoxidase method to detect HTT with anti-HTT1–17 (Ab1). Boxed regions of the cingulate cortex and the putamen are shown in images to the right of each section. HTT immunoreactivity has a strong somatodendritic localization in WT and TgHD cortex and in somata of medium sized neostriatal neurons. There is no obvious difference in labeling between WT and TgHD neurons. Scale bars 100 μm.

DARPP32 is highly localized to neuronal cell bodies and processes of the normal rodent and human neostriatum. A decline in DARPP32 immunoreactivity in the neostriatum is characteristic of HD mice [73, 74]. Immunoperoxidase labeling for DARPP32 in the neostriatum of F2 generation 16 month old WT and TgHD minipigs showed intense labeling in neuronal cell bodies and neuropil (Fig. 8A–D). Some areas of less intense DARPP32 neuropil staining were present and may be striosomes, which have been described using other neuronal markers in rodent and human striatum [75, 76] (Fig. 8B, D). Immunofluorescence analysis of caudate and putamen of F2 WT and TgHD minipigs at ages 4, 10 and 16 months also showed DARPP32 robustly expressed in neostriatal neurons and neuropil (Fig. 9A–C, shown for 16 months). A quantitative stereology analysis was performed in the sibling pair of 16 month old minipigs. Results showed that the median number of DARPP32 + neurons per mm^3 in caudate and putamen of the TgHD minipig was slightly lower compared to the WT (TgHD: 24,781 caudate neurons and 22,351 putamen neurons, and WT: 26,846 caudate

neurons and 23,863 putamen neurons) (Fig. 9C). In the TgHD brain there were reduced signal intensities for DARPP32 labeling in the caudate nucleus (11.3% reduction) and putamen (31.7% reduction) compared to the WT sibling. Although these data are highly preliminary and need confirmation in additional minipigs, the results suggest that by 16 months of age the levels of DARPP32 in TgHD minipig start to decline.

Analysis of reproductive capacity in TgHD boars

The number of spermatozoa per ejaculate was systematically evaluated in the transgenic boars from the age of 13 months to 26 months. There was a significant decline in the median number of spermatozoa in TgHD minipigs ($2.45–3.65 \times 10^9$ of spermatozoa) compared to WT ($8.15–12.48 \times 10^9$ of spermatozoa) (Fig. 10A, Kruskal-Wallis test $p < 0.001$ followed by *post-hoc* Mann-Whitney U, $p < 0.01$).These data suggest an impairment of spermatogenic production of the testes of TgHD minipigs. A time course analysis of the TgHD sperm samples showed that sperm number was reduced at 13 months and remained low up to 26 months (Supplementary Data S8). IVF assay showed that in WT oocytes with zona pellucida intact, the number of TgHD spermatozoa that penetrated the oocyte was lower than for the WT spermatozoa (Fig. 10B). The median percentage of WT oocytes that were penetrated by TgHD spermatozoa was significantly lower than WT oocytes penetrated by WT spermatozoa (Kruskal-Wallis test $p < 0.001$ followed by *post-hoc* Mann-Whitney U, $p < 0.05$) (Fig. 10C). These results indicated that the penetration activity of spermatozoa in TgHD boars was impaired compared to those of WT spermatozoa. To investigate the basis for the impaired penetration rate in TgHD, WT oocytes with zona pellucida removed were used for further analysis. Removing the zona pellucida markedly increased penetration rate in the WT and TgHD groups to 100% level (Fig. 10D). These findings suggest that the presence of the HTT gene interferes with the penetration of TgHD spermatozoa through the zona pellucida but does not

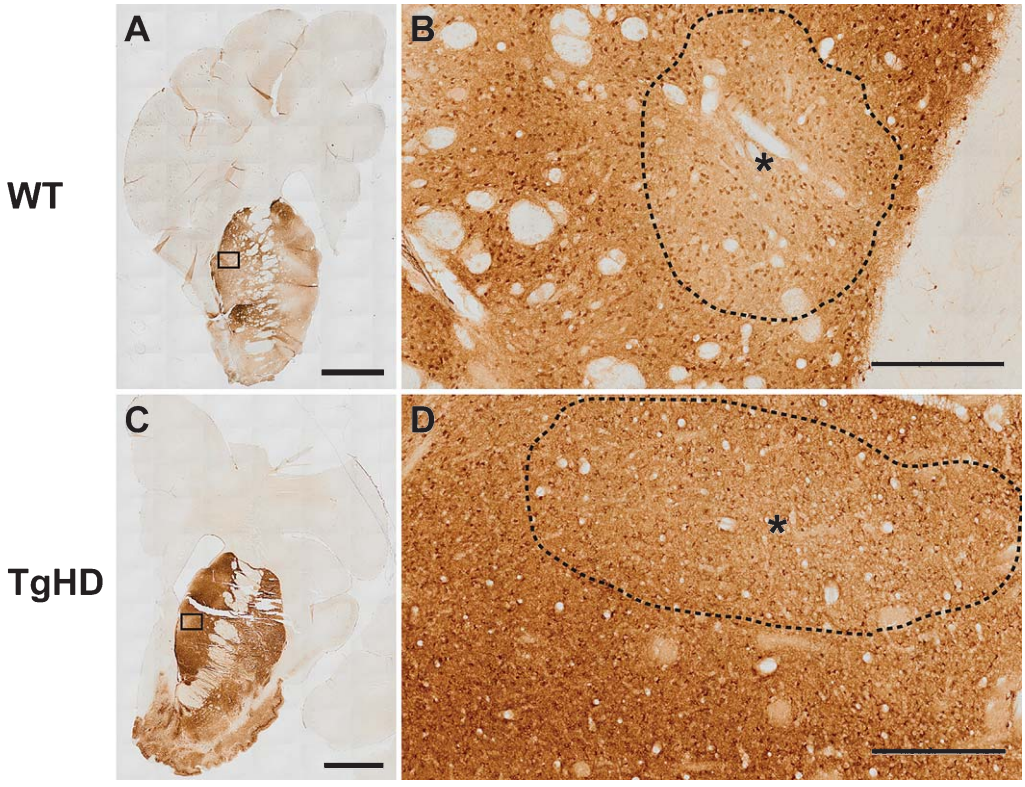

Fig. 8. DARPP32 immunoreactivity with immunoperoxidase method in 16 month old F2 WT and TgHD minipig brain. (A and C) Coronal sections through the neostriatum of WT (A) and TgHD (C) minipig show intense labeling for DARPP32 in the caudate nucleus and putamen and in the basal forebrain. Boxed areas are shown at higher magnification in B and D. (B and D) Higher magnification images show the intense labeling of neuropil and cell bodies. Areas of weaker neuropil labeling are demarcated by a dashed line and asterisk in the center and may represent striosomes. Scale bars in A and C are 5 mm and in B and D are 500 μm.

interfere with fusion of the post-acrosomal spermatozoa membrane and the cytoplasmic membrane of oocytes.

DISCUSSION

Rodent models of HD including transgenic mice expressing N-terminal fragments of mutant HTT have been very important for understanding disease mechanisms, validating targets, and testing candidate therapies, but have some limitations for modeling the human disease [2, 17]. The miniature pig (*Sus scrofa*) has similarities to humans in anatomy, physiology, and metabolism [20, 28, 29]. The size and structure of pig brain makes it amenable to neurosurgical procedures and non-invasive high resolution neuroimaging methods similar to those performed in humans [30, 34, 77]. The lifespan of minipigs and their sophisticated cognitive and motor abilities also make them useful for long-term studies of learning, memory and behavior [28, 78, 79]. In this study we show successful establishment of a transgenic minipig stably expressing N-truncated human mutant huntingtin 1–548 with 124 glutamines through multiple generations.

Transgenic HD minipigs were generated using lentiviral transduction of porcine zygotes in syngamy, at the onset of embryonic DNA synthesis. The precise timing of lentiviral transduction enhances incorporation of the transgene cDNA into embryos. The lentiviral delivery did not cause mosaicism, since the mutant HTT was revealed in all tissues tested in F1 and F2 TgHD minipigs and maintained the same number of glutamines. We found an in-frame deletion of the expanded CAG/CAA tract such that the integrated transgene encoded 124 glutamines instead of the original 145 glutamines. Similar contraction of the polyglutamine repeat has been observed in human HD [80]. The rates of transgenesis and viability of offspring in pig were higher with lentiviral delivery than with a cloning strategy reported previously [55, 81, 82]. In our experiments, the lentiviral construct that was used to transduce the minipig genome did not influence survival or normal development through multiple generations. The total neonatal mortality of our TgHD minipigs was 17.2%, which is in the range of the WT strain (16.4%, Supplementary Data S6). In contrast, the transgenic HD pigs, generated via a cloning strategy and bearing N-terminal mutant HTT (208 amino acids and 105 Q), showed a severe chorea phenotype before death and the presence of apoptotic cells in brain [55].

Both female and male transmissions of the HD transgene were confirmed in our TgHD minipigs. Two litters of F1 generation minipigs were born with a rate of transgenesis of 29.4%. The litters of F2 and F3 generations had a Mendelian inheritance of the transgene of 40.2% and 34.9%, respectively. Importantly, one single copy of exogenous HTT was found in chromosome 1 (1q24-q25) where it was maintained in F1 and F2 offspring. The TgHD minipigs of F0 –F2 generations had two alleles coding endogenous pig HTT and one allele for the N-terminal human mutant HTT. No homozygote TgHD minipigs were generated with heterozygote TgHD matings. The site of insertion of the transgene may have disrupted some essential genetic sequence that caused lethality of progeny homozygous for the HD transgene [83]. More detailed information on the exact site of insertion of the transgene in chromosome 1 may reveal more insights about potential homozygote lethality.

Mutant HTT protein expression was detected in different brain regions including cortex, caudate nucleus and putamen and in a variety of peripheral tissues and confirmed by both Western Blot analysis and TR-FRET. With one exception (hypothalamus in one of the TgHD minipigs), the data from WB and TR-FRET biochemical assays showed a good correspondence for the relative distribution of human mutant HTT in different brain regions and peripheral tissues. The expression of the transgenic protein was not confirmed in heart, stomach, spleen and skeletal muscle. *Trottier* et al. [84] determined the presence of HTT protein also in heart. Discrepancies in observed distribution of huntingtin in tissues can be influenced by the preparation of protein lysates [85]. In "bloody" tissues (liver, spleen), red color of analyte is known to artificially increase background in TR-FRET readout thus higher mutant HTT background signals in these WT tissues were likely due to this effect. The variations in the expression level of protein were expected in skin tissue due to insufficient homogenization.

Midbrain dopaminergic neurons play a critical role in basal ganglia circuitry and function including coordination of movement. Protein phosphatase 1 regulatory subunit 1B, also known as dopamine- and cAMP-regulated neuronal phosphoprotein (DARPP32), is highly expressed in caudate-putamen medium-sized spiny neurons [73, 86]. Dopamine D1 receptor stimulation enhances cyclic AMP formation, resulting in the phosphorylation of DARPP32 [86] at Thr34 by PKA [87]. A loss of DARPP32 levels in medium-sized spiny striatal neurons was observed in several rodent models of HD [74, 88], and in the globus pallidus and putamen

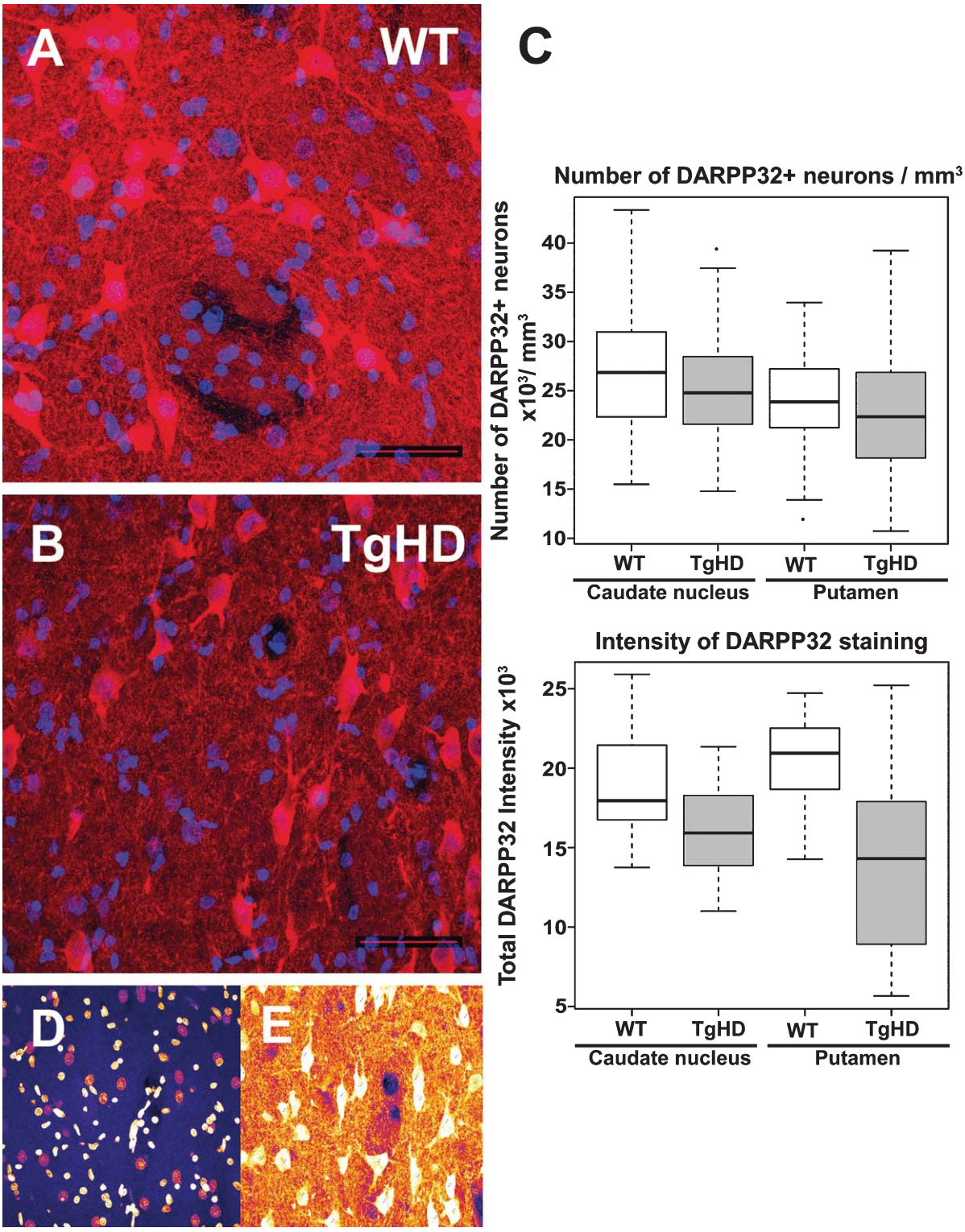
A
WT
B
TgHD
D
E
C
Number of DARPP32+ neurons / mm³
Number of DARPP32+ neurons x10³/ mm³
40
35
30
25
20
15
10
WT
TgHD
WT
TgHD
Caudate nucleus
Putamen
Intensity of DARPP32 staining
Total DARPP32 Intensity x10³
25
20
15
10
5
WT
TgHD
WT
TgHD
Caudate nucleus
Putamen

Fig. 9.

of 7 month old HD sheep [21]. A 16 month old TgHD minipig brain had a reduction compared to WT in the intensity of neuronal labeling for DARPP32 in the caudate nucleus and putamen. Clearly these findings, which are based on a detailed quantitative analysis of only one sibling pair of WT and TgHD minipigs, need to be confirmed in more animals. Nevertheless, the data suggest that changes in DARPP32 may begin in the TgHD minipig brain at around 16 months of age.

The formation of aggregates is a hallmark of HD pathology. Nuclear and cytoplasmic inclusions of mutant HTT are seen in human postmortem HD brain and in mouse models of HD [9, 72]. There was no evidence of aggregates of mutant HTT protein in the TgHD minipig up to 16 months of age based on biochemical (AGERA, filter retardation) and immunohistochemical assays with antibody to anti-HTT1-17. This antibody detects mutant HTT inclusions in the human HD brain. Other antibodies commonly used to detect nuclear inclusions of human HTT fragments in HD mice including MW8 and EM48 produced no staining in the TgHD minipigs. The absence of nuclear inclusions in the TgHD minipigs was consistent with the negative results for aggregation observed using the AGERA and filter retardations assays. Clearly study of brains from older TgHD minipigs will be needed to determine onset of aggregate formation. Many factors influence the incidence of aggregated mutant HTT including levels of mutant protein expression, polyglutamine length, the length of the mutant HTT fragment, and age of the animal [89–91]. It is noteworthy that a well studied HD mouse model BACHD which expresses full length mutant HTT with 97 glutamines encoded by CAG/CAA repeats [92] develops brain pathology and progressive motor deficits but lacks obvious intranuclear mutant HTT aggregates [93]. Some neuropil aggregates appeared in late stages (12–18 months BACHD) and were more prominent when aggressive antigen retrieval and anti-HTT antibody 3B5H10 were used in the brain sections [94], suggesting that epitopes for detecting mutant HTT aggregates may be masked. As with BACHD, the polyglutamine tract in our TgHD minipig has a mix of CAG/CAA repeats. It is possible that CAG/CAA sequence generates protein conformations that are unfavorable for immunodetection of aggregates.

A surprising finding was evidence for a decline in fertility in F1 boars caused by reduced sperm number and penetration rate. This phenotype can be easily monitored in the TgHD minipigs and therefore represents a biomarker that can be suitable for therapeutics. From 13–26 months the decline in sperm function was constant. Analysis of earlier ages might reveal a period of progressive decline that could also be a useful index for analysis of therapeutics. As only 2 F1 transgenic boars were available for detailed analysis, these findings must be considered preliminary and we are currently investigating reproductive competence in a larger cohort of F2 animals. Pathology in the germinal epithelium has been documented in human HD and YAC 128 HD mouse on histological sections where a decreased number of germ cells and reduced seminiferous tubule cross-sectional area have been observed [95]. The testicular pathology in humans was related to the presence of mutant HTT since severity was greater in patients with longer CAG repeats and testicular pathology was not present in a patient with amyotrophic lateral sclerosis. The YAC 128 HD mouse develops testicular pathology between 9 and 12 months prior to significant reduction in testosterone or GnRH levels but coinciding with changes in the brain and the appearance of motor deficits. Unlike the TgHD minipigs, problems with sperm quality and fertility have not been reported in HD patients.

No evident changes in motor function were observed in a F0 TgHD minipig up to the age of 40 months. However, only 4 animals (3 TG vs. 1 WT) were subjected to the study. A systematic quantitative study focusing on changes in motor and cognitive functions in TgHD minipigs is underway (Dr. R. Reilmann, unpublished data). In contrast to our TgHD minipigs, the short-lived transgenic piglets produced by a cloning strategy showed dyskinesia and chorea-like movements before death [55].

In summary we have developed a heterozygote TgHD minipig that expresses a human mutant HTT fragment throughout the CNS and peripheral tissues in a stable fashion through multiple generations. The TgHD minipig is healthy at birth and through early

Fig. 9. Immunofluorescence labeling of DARPP32 in WT and TgHD minipig neostriatum. (A and B) Shown are images of microscopic fields from the putamen of 16 month old WT (A) and TgHD sibling minipig (B). DARPP32 labeling in the cytoplasm is red and DAPI staining in the nucleus is in blue. (C) Upper boxplot shows median numbers of DARPP32 + neurons (mm^3) in caudate nucleus and putamen of WT and TgHD minipigs. Lower box plots shows median intensity of DARPP32 staining determined as described in Methods. (D) and (E) are pseudo-color images of DAPI stained nuclei and DARPP32 stained neurons respectively in WT putamen obtained using fire view in FiJi software as part of thresholding for the neuronal counting procedure. Scale bar 50 μm. (Colours are visible in the online version of the article; http://dx.doi.org/10.3233/JHD-130001)

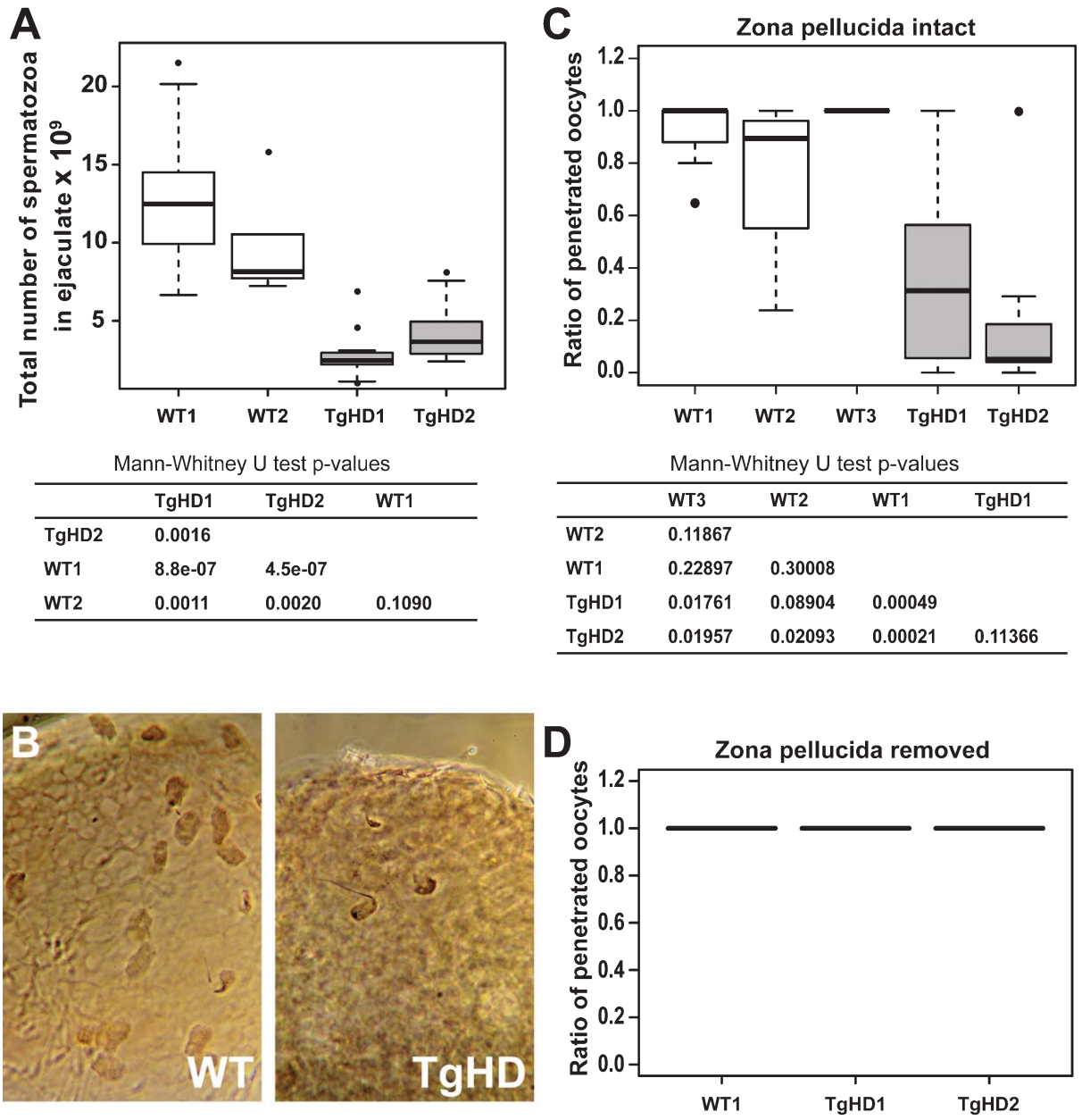

Mann-Whitney U test p-values

	TgHD1	TgHD2	WT1
TgHD2	0.0016		
WT1	8.8e-07	4.5e-07	
WT2	0.0011	0.0020	0.1090

Mann-Whitney U test p-values

	WT3	WT2	WT1	TgHD1
WT2	0.11867			
WT1	0.22897	0.30008		
TgHD1	0.01761	0.08904	0.00049	
TgHD2	0.01957	0.02093	0.00021	0.11366

Fig. 10. Failure of reproductive capacity in TgHD boars. (A) Boxplots show number of spermatozoa per ejaculate in two WT boars and in 2 TgHD minipig boars of similar age (see methods for details). The median number of spermatozoa is reduced in TgHD minipigs compared to WT minipigs, *p*-values for all pairwise comparisons (Mann-Whitney U test) are shown in the table. (B) Left: Image of WT oocyte fertilized with WT spermatozoa *in vitro*: Note the large number of penetrated, partly de-condensed spermatozoa that are visible in intact oocyte *in vitro* fertilized with WT spermatozoa. Right: Image of WT oocyte fertilized with TgHD spermatozoa *in vitro*. Note the small number of spermatozoa. The syngamy of male and female pronuclei is visible and only one supernumerary penetrated sperm is evident. (C) Boxplots show the median ratio of intact WT oocytes (including zona pellucida) penetrated by WT or TgHD spermatozoa as determined by IVF. *P*-values for all pairwise comparisons (Mann-Whitney U test) are shown in the table below. (D) Boxplots show the median ratio of WT oocytes with zona pellucida removed penetrated by WT or TgHD spermatozoa as determined by IVF.

development and does not exhibit obvious signs of abnormal movement up to 40 months of age. However, a decline is evident at 16 months in DARPP32 immunoreactivity in the neostriatum, the region most affected in HD, as well as a decline in sperm number and penetration rate beginning at about 13 months. Formal testing of the TgHD minipigs in a battery of motor tasks is now underway.

ACKNOWLEDGMENTS

We would like to thank Patricia Jandurova, Irena Deylova and Stepan Hladky for the excellent technical assistance. We are grateful to Professor Jindrich Martinek for his help with the immunohistochemistry and virtual microscopy. We thank Jiri Jarkovsky, Institute of Biostatistics, Masaryk University, Brno, Czech Republic for advice on statistics. This work was supported by the CHDI Foundation (ID 1035), The Technical Agency of the Czech Republic (TA01011466), the project EXAM from European Regional Development Fund CZ.1.05/2.1.00/03.0124, The Grant Agency of the Charles University - Project No. 589412 and RVO 67985904.

CONFLICT OF INTEREST

One of the authors, Dr. David S. Howland is employed by CHDI Inc. which supported this research.

REFERENCES

[1] Gil JM, Rego AC. Mechanisms of neurodegeneration in Huntington's disease. The European Journal of Neuroscience. 2008;27(11):2803-20. PubMed PMID: 18588526. Epub 2008/07/01. eng.

[2] Zuccato C, Valenza M, Cattaneo E. Molecular mechanisms and potential therapeutical targets in Huntington's disease. Physiological Reviews. 2010;90(3):905-81. PubMed PMID: 20664076. Epub 2010/07/29. eng.

[3] Perez-De La Cruz V, Santamaria A. Integrative hypothesis for Huntington's disease: A brief review of experimental evidence. Physiological Research/Academia Scientiarum Bohemoslovaca. 2007;56(5):513-26. PubMed PMID: 17184144. Epub 2006/12/23. eng.

[4] Walker FO. Huntington's disease. Lancet. 2007;369(9557): 218-28. PubMed PMID: 17240289. Epub 2007/01/24. eng.

[5] The Huntington's Disease Collaborative Research Group. A novel gene containing a trinucleotide repeat that is expanded and unstable on Huntington's disease chromosomes. Cell. 1993;72(6):971-83. PubMed PMID: 8458085. Epub 1993/03/26. eng.

[6] Brinkman RR, Mezei MM, Theilmann J, Almqvist E, Hayden MR. The likelihood of being affected with Huntington disease by a particular age, for a specific CAG size. American Journal of Human Genetics. 1997;60(5):1202-10. PubMed PMID: 9150168. Pubmed Central PMCID: 1712445. Epub 1997/05/01. eng.

[7] Dunnett SB, Rosser AE. Cell transplantation for Huntington's disease Should we continue? Brain Research Bulletin. 2007;72(2-3):132-47. PubMed PMID: 17352937. Epub 2007/03/14. eng.

[8] Lee ST, Kim M. Aging and neurodegeneration. Molecular mechanisms of neuronal loss in Huntington's disease. Mechanisms of Ageing and Development. 2006;127(5):432-5. PubMed PMID: 16527334. Epub 2006/03/11. eng.

[9] Davies SW, Turmaine M, Cozens BA, DiFiglia M, Sharp AH, Ross CA, et al. Formation of neuronal intranuclear inclusions underlies the neurological dysfunction in mice transgenic for the HD mutation. Cell. 1997;90(3):537-48. PubMed PMID: 9267033. Epub 1997/08/08. eng.

[10] Mangiarini L, Sathasivam K, Seller M, Cozens B, Harper A, Hetherington C, et al. Exon 1 of the HD gene with an expanded CAG repeat is sufficient to cause a progressive neurological phenotype in transgenic mice. Cell. 1996;87(3):493-506. PubMed PMID: 8898202. Epub 1996/11/01. eng.

[11] Schilling G, Becher MW, Sharp AH, Jinnah HA, Duan K, Kotzuk JA, et al. Intranuclear inclusions and neuritic aggregates in transgenic mice expressing a mutant N-terminal fragment of huntingtin. Human Molecular Genetics. 1999; 8(3):397-407. PubMed PMID: 9949199. Epub 1999/02/09. eng.

[12] Reddy PH, Williams M, Charles V, Garrett L, Pike-Buchanan L, Whetsell WO, Jr., et al. Behavioural abnormalities and selective neuronal loss in HD transgenic mice expressing mutated full-length HD cDNA. Nature Genetics. 1998; 20(2):198-202. PubMed PMID: 9771716. Epub 1998/10/15. eng.

[13] Van Raamsdonk JM, Murphy Z, Slow EJ, Leavitt BR, Hayden MR. Selective degeneration and nuclear localization of mutant huntingtin in the YAC128 mouse model of Huntington disease. Human molecular genetics. 2005;14(24):3823-35. PubMed PMID: 16278236. Epub 2005/11/10. eng.

[14] Ariano MA, Aronin N, Difiglia M, Tagle DA, Sibley DR, Leavitt BR, et al. Striatal neurochemical changes in transgenic models of Huntington's disease. Journal of Neuroscience Research. 2002;68(6):716-29. PubMed PMID: 12111832. Epub 2002/07/12. eng.

[15] Reynolds GP, Dalton CF, Tillery CL, Mangiarini L, Davies SW, Bates GP. Brain neurotransmitter deficits in mice transgenic for the Huntington's disease mutation. Journal of Neurochemistry. 1999;72(4):1773-6. PubMed PMID: 10098889. Epub 1999/03/31. eng.

[16] Van Raamsdonk JM, Pearson J, Slow EJ, Hossain SM, Leavitt BR, Hayden MR. Cognitive dysfunction precedes neuropathology and motor abnormalities in the YAC128 mouse model of Huntington's disease. The Journal of Neuroscience : The Official Journal of the Society for Neuroscience. 2005;25(16):4169-80. PubMed PMID: 15843620. Epub 2005/04/22. eng.

[17] Yang SH, Chan AW. Transgenic animal models of huntington's disease. Current Topics in Behavioral Neurosciences. 2011;7:61-85. PubMed PMID: 21225414. Epub 2011/01/13. eng.

[18] Bendixen E, Danielsen M, Larsen K, Bendixen C. Advances in porcine genomics and proteomics–a toolbox for developing the pig as a model organism for molecular biomedical research. Briefings in Functional Genomics. 2010;9(3):208-19. PubMed PMID: 20495211. Epub 2010/05/25. eng.

[19] Casal M, Haskins M. Large animal models and gene therapy. Eur J Hum Genet. 2006;14(3):266-72. PubMed PMID: 16333317. Epub 2005/12/08. eng.

[20] Swindle MM, Makin A, Herron AJ, Clubb FJ, Jr., Frazier KS. Swine as models in biomedical research and toxicology testing. Vet Pathol. 2012;49(2):344-56. PubMed PMID: 21441112. Epub 2011/03/29. eng.

[21] Jacobsen JC, Bawden CS, Rudiger SR, McLaughlan CJ, Reid SJ, Waldvogel HJ, et al. An ovine transgenic Huntington's disease model. Human Molecular Genetics. 2010; 19(10):1873-82. PubMed PMID: 20154343. Pubmed Central PMCID: 2860888. Epub 2010/02/16. eng.

[22] Yang SH, Cheng PH, Banta H, Piotrowska-Nitsche K, Yang JJ, Cheng EC, et al. Towards a transgenic model

of Huntington's disease in a non-human primate. Nature. 2008;453(7197):921-4. PubMed PMID: 18488016. Pubmed Central PMCID: 2652570. Epub 2008/05/20. eng.

[23] Bjarkam CR, Jorgensen RL, Jensen KN, Sunde NA, Sorensen JC. Deep brain stimulation electrode anchoring using BioGlue((R)), a protective electrode covering, and a titanium microplate. Journal of Neuroscience Methods. 2008; 168(1):151-5. PubMed PMID: 17953993. Epub 2007/10/24. eng.

[24] Ettrup KS, Sorensen JC, Rodell A, Alstrup AK, Bjarkam CR. Hypothalamic deep brain stimulation influences autonomic and limbic circuitry involved in the regulation of aggression and cardiocerebrovascular control in the Gottingen minipig. Stereotactic and Functional Neurosurgery. 2012;90(5):281-91. PubMed PMID: 22797692. Epub 2012/07/17. eng.

[25] Fjord-Larsen L, Kusk P, Tornoe J, Juliusson B, Torp M, Bjarkam CR, et al. Long-term delivery of nerve growth factor by encapsulated cell biodelivery in the Gottingen minipig basal forebrain. Molecular Therapy : The Journal of the American Society of Gene Therapy. 2010;18(12):2164-72. PubMed PMID: 20664524. Pubmed Central PMCID: 2997581. Epub 2010/07/29. eng.

[26] Jensen KN, Deding D, Sorensen JC, Bjarkam CR. Long-term implantation of deep brain stimulation electrodes in the pontine micturition centre of the Gottingen minipig. Acta Neurochirurgica. 2009;151(7):785-94; discussion 94. PubMed PMID: 19404572. Epub 2009/05/01. eng.

[27] Lind NM, Moustgaard A, Jelsing J, Vajta G, Cumming P, Hansen AK. The use of pigs in neuroscience: Modeling brain disorders. Neuroscience and Biobehavioral Reviews. 2007; 31(5):728-51. PubMed PMID: 17445892. Epub 2007/04/21. eng.

[28] Lunney JK. Advances in swine biomedical model genomics. International Journal of Biological Sciences. 2007;3(3):179-84. PubMed PMID: 17384736. Pubmed Central PMCID: 1802015. Epub 2007/03/27. eng.

[29] Vodicka P, Smetana K, Jr., Dvorankova B, Emerick T, Xu YZ, Ourednik J, et al. The miniature pig as an animal model in biomedical research. Annals of the New York Academy of Sciences. 2005;1049:161-71. PubMed PMID: 15965115. Epub 2005/06/21. eng.

[30] Ishizu K, Smith DF, Bender D, Danielsen E, Hansen SB, Wong DF, et al. Positron emission tomography of radioligand binding in porcine striatum *in vivo*: Haloperidol inhibition linked to endogenous ligand release. Synapse. 2000; 38(1):87-101. PubMed PMID: 10941144. Epub 2000/08/15. eng.

[31] Rosa-Neto P, Doudet DJ, Cumming P. Gradients of dopamine D1- and D2/3-binding sites in the basal ganglia of pig and monkey measured by PET. NeuroImage. 2004;22(3):1076-83. PubMed PMID: 15219579. Epub 2004/06/29. eng.

[32] Andersen F, Watanabe H, Bjarkam C, Danielsen EH, Cumming P, DaNe XSG. Pig brain stereotaxic standard space: Mapping of cerebral blood flow normative values and effect of MPTP-lesioning. Brain Research Bulletin. 2005;66(1):17-29. PubMed PMID: 15925140. Epub 2005/06/01. eng.

[33] Duhaime AC, Saykin AJ, McDonald BC, Dodge CP, Eskey CJ, Darcey TM, et al. Functional magnetic resonance imaging of the primary somatosensory cortex in piglets. Journal of Neurosurgery. 2006;104(4 Suppl):259-64. PubMed PMID: 16619637. Epub 2006/04/20. eng.

[34] Gizewski ER, Schanze T, Bolle I, de Greiff A, Forsting M, Laube T. Visualization of the visual cortex in minipigs using fMRI. Research in Veterinary Science. 2007;82(3):281-6. PubMed PMID: 17064742. Epub 2006/10/27. eng.

[35] Watanabe H, Andersen F, Simonsen CZ, Evans SM, Gjedde A, Cumming P, et al. MR-based statistical atlas of the Gottingen minipig brain. NeuroImage. 2001;14(5):1089-96. PubMed PMID: 11697940. Epub 2001/11/08. eng.

[36] Bjarkam CR, Cancian G, Larsen M, Rosendahl F, Ettrup KS, Zeidler D, et al. A MRI-compatible stereotaxic localizer box enables high-precision stereotaxic procedures in pigs. Journal of Neuroscience Methods. 2004;139(2):293-8. PubMed PMID: 15488243. Epub 2004/10/19. eng.

[37] Rosendal F, Chakravarty MM, Sunde N, Rodell A, Jonsdottir KY, Pedersen M, et al. Defining the intercommissural plane and stereotactic coordinates for the Basal Ganglia in the Gottingen minipig brain. Stereotactic and Functional Neurosurgery. 2010;88(3):138-46. PubMed PMID: 20357521. Epub 2010/04/02. eng.

[38] Rosendal F, Frandsen J, Chakravarty MM, Bjarkam CR, Pedersen M, Sangill R, et al. New surgical technique reduces the susceptibility artefact at air-tissue interfaces on *in vivo* cerebral MRI in the Gottingen minipig. Brain Research Bulletin. 2009;80(6):403-7. PubMed PMID: 19712728. Epub 2009/08/29. eng.

[39] Rosendal F, Pedersen M, Sangill R, Stodkilde-Jorgensen H, Nielsen MS, Bjarkam CR, et al. MRI protocol for *in vivo* visualization of the Gottingen minipig brain improves targeting in experimental functional neurosurgery. Brain Research Bulletin. 2009;79(1):41-5. PubMed PMID: 19185604. Epub 2009/02/03. eng.

[40] Archibald AL, Bolund L, Churcher C, Fredholm M, Groenen MA, Harlizius B, et al. Pig genome sequence–analysis and publication strategy. BMC Genomics. 2010;11:438. PubMed PMID: 20642822. Pubmed Central PMCID: 3017778. Epub 2010/07/21. eng.

[41] Jiang Z, Rothschild MF. Swine genome science comes of age. International Journal of Biological Sciences. 2007;3(3):129-31. PubMed PMID: 17384732. Pubmed Central PMCID: 1802017. Epub 2007/03/27. eng.

[42] Jorgensen FG, Hobolth A, Hornshoj H, Bendixen C, Fredholm M, Schierup MH. Comparative analysis of protein coding sequences from human, mouse and the domesticated pig. BMC Biology. 2005;3:2. PubMed PMID: 15679890. Pubmed Central PMCID: 549206. Epub 2005/02/01. eng.

[43] Wernersson R, Schierup MH, Jorgensen FG, Gorodkin J, Panitz F, Staerfeldt HH, et al. Pigs in sequence space: A 0.66X coverage pig genome survey based on shotgun sequencing. BMC Genomics. 2005;6:70. PubMed PMID: 15885146. Pubmed Central PMCID: 1142312. Epub 2005/05/12. eng.

[44] Ramos AM, Crooijmans RP, Affara NA, Amaral AJ, Archibald AL, Beever JE, et al. Design of a high density SNP genotyping assay in the pig using SNPs identified and characterized by next generation sequencing technology. PloS One. 2009;4(8):e6524. PubMed PMID: 19654876. Pubmed Central PMCID: 2716536. Epub 2009/08/06. eng.

[45] Kim J, Cho IS, Hong JS, Choi YK, Kim H, Lee YS. Identification and characterization of new microRNAs from pig. Mammalian Genome : Official Journal of the International Mammalian Genome Society. 2008;19(7-8):570-80. PubMed PMID: 18548309. Epub 2008/06/13. eng.

[46] Li M, Xia Y, Gu Y, Zhang K, Lang Q, Chen L, et al. MicroRNAome of porcine pre- and postnatal development. PloS One. 2010;5(7):e11541. PubMed PMID: 20634961. Pubmed Central PMCID: 2902522. Epub 2010/07/17. eng.

[47] Reddy AM, Zheng Y, Jagadeeswaran G, Macmil SL, Graham WB, Roe BA, et al. Cloning, characterization and

expression analysis of porcine microRNAs. BMC Genomics. 2009;10:65. PubMed PMID: 19196471. Pubmed Central PMCID: 2644714. Epub 2009/02/07. eng.

[48] Hofmann A, Kessler B, Ewerling S, Weppert M, Vogg B, Ludwig H, et al. Efficient transgenesis in farm animals by lentiviral vectors. EMBO Reports. 2003;4(11):1054-60. PubMed PMID: 14566324. Pubmed Central PMCID: 1326377. Epub 2003/10/21. eng.

[49] Nagashima H, Fujimura T, Takahagi Y, Kurome M, Wako N, Ochiai T, et al. Development of efficient strategies for the production of genetically modified pigs. Theriogenology. 2003;59(1):95-106. PubMed PMID: 12499021. Epub 2002/12/25. eng.

[50] Kurome M, Ueda H, Tomii R, Naruse K, Nagashima H. Production of transgenic-clone pigs by the combination of ICSI-mediated gene transfer with somatic cell nuclear transfer. Transgenic Research. 2006;15(2):229-40. PubMed PMID: 16604463. Epub 2006/04/11. eng.

[51] Lavitrano M, Busnelli M, Cerrito MG, Giovannoni R, Manzini S, Vargiolu A. Sperm-mediated gene transfer. Reproduction, Fertility, and Development. 2006;18(1-2):19-23. PubMed PMID: 16478599. Epub 2006/02/16. eng.

[52] Matsuyama N, Hadano S, Onoe K, Osuga H, Showguchi-Miyata J, Gondo Y, et al. Identification and characterization of the miniature pig Huntington's disease gene homolog: Evidence for conservation and polymorphism in the CAG triplet repeat. Genomics. 2000;69(1):72-85. PubMed PMID: 11013077. Epub 2000/10/03. eng.

[53] Lin B, Rommens JM, Graham RK, Kalchman M, MacDonald H, Nasir J, et al. Differential 3′ polyadenylation of the Huntington disease gene results in two mRNA species with variable tissue expression. Human Molecular Genetics. 1993;2(10):1541-5. PubMed PMID: 7903579. Epub 1993/10/01. eng.

[54] Aigner B, Renner S, Kessler B, Klymiuk N, Kurome M, Wunsch A, et al. Transgenic pigs as models for translational biomedical research. Journal of Molecular Medicine. 2010; 88(7):653-64. PubMed PMID: 20339830. Epub 2010/03/27. eng.

[55] Yang D, Wang CE, Zhao B, Li W, Ouyang Z, Liu Z, et al. Expression of Huntington's disease protein results in apoptotic neurons in the brains of cloned transgenic pigs. Human Molecular Genetics. 2010;19(20):3983-94. PubMed PMID: 20660116. Pubmed Central PMCID: 2947404. Epub 2010/07/28. eng.

[56] Motlik J, Klima J, Dvorankova B, Smetana K, Jr. Porcine epidermal stem cells as a biomedical model for wound healing and normal/malignant epithelial cell propagation. Theriogenology. 2007;67(1):105-11. PubMed PMID: 17055565. Epub 2006/10/24. eng.

[57] Trask BJ. DNA sequence localization in metaphase and interphase cells by fluorescence *in situ* hybridization. Methods in Cell Biology. 1991;35:3-35. PubMed PMID: 1779860. Epub 1991/01/01. eng.

[58] Ruijter JM, Ramakers C, Hoogaars WM, Karlen Y, Bakker O, van den Hoff MJ, et al. Amplification efficiency: Linking baseline and bias in the analysis of quantitative PCR data. Nucleic Acids Research. 2009;37(6):e45. PubMed PMID: 19237396. Pubmed Central PMCID: 2665230. Epub 2009/02/25. eng.

[59] DiFiglia M, Sapp E, Chase K, Schwarz C, Meloni A, Young C, et al. Huntingtin is a cytoplasmic protein associated with vesicles in human and rat brain neurons. Neuron. 1995; 14(5):1075-81. PubMed PMID: 7748555. Epub 1995/05/01. eng.

[60] Weiss A, Klein C, Woodman B, Sathasivam K, Bibel M, Regulier E, et al. Sensitive biochemical aggregate detection reveals aggregation onset before symptom development in cellular and murine models of Huntington's disease. Journal of Neurochemistry. 2008;104(3):846-58. PubMed PMID: 17986219. Epub 2007/11/08. eng.

[61] Legleiter J, Mitchell E, Lotz GP, Sapp E, Ng C, DiFiglia M, et al. Mutant huntingtin fragments form oligomers in a polyglutamine length-dependent manner *in vitro* and *in vivo*. The Journal of Biological Chemistry. 2010;285(19):14777-90. PubMed PMID: 20220138. Pubmed Central PMCID: 2863238. Epub 2010/03/12. eng.

[62] Sontag EM, Lotz GP, Agrawal N, Tran A, Aron R, Yang G, et al. Methylene blue modulates huntingtin aggregation intermediates and is protective in Huntington's disease models. The Journal of Neuroscience : The Official Journal of the Society for Neuroscience. 2012;32(32):11109-19. PubMed PMID: 22875942. Epub 2012/08/10. eng.

[63] Sontag EM, Lotz GP, Yang G, Sontag CJ, Cummings BJ, Glabe CG, et al. Detection of mutant huntingtin aggregation conformers and modulation of SDS-soluble fibrillar oligomers by small molecules. Journal of Huntington's Disease. 2012;1(1):127-40.

[64] Scherzinger E, Lurz R, Turmaine M, Mangiarini L, Hollenbach B, Hasenbank R, et al. Huntingtin-encoded polyglutamine expansions form amyloid-like protein aggregates *in vitro* and *in vivo*. Cell. 1997;90(3):549-58. PubMed PMID: 9267034. Epub 1997/08/08. eng.

[65] Weiss A, Abramowski D, Bibel M, Bodner R, Chopra V, DiFiglia M, et al. Single-step detection of mutant huntingtin in animal and human tissues: A bioassay for Huntington's disease. Analytical Biochemistry. 2009;395(1):8-15. PubMed PMID: 19664996. Epub 2009/08/12. eng.

[66] Bjarkam CR, Pedersen M, Sorensen JC. New strategies for embedding, orientation and sectioning of small brain specimens enable direct correlation to MR-images, brain atlases, or use of unbiased stereology. Journal of Neuroscience Methods. 2001;108(2):153-9. PubMed PMID: 11478974. Epub 2001/08/02. eng.

[67] Sorensen JC, Bjarkam CR, Danielsen EH, Simonsen CZ, Geneser FA. Oriented sectioning of irregular tissue blocks in relation to computerized scanning modalities: Results from the domestic pig brain. Journal of Neuroscience Methods. 2000;104(1):93-8. PubMed PMID: 11163415. Epub 2001/02/13. eng.

[68] Guzowski JF, McNaughton BL, Barnes CA, Worley PF. Environment-specific expression of the immediate-early gene Arc in hippocampal neuronal ensembles. Nature Neuroscience. 1999;2(12):1120-4. PubMed PMID: 10570490. Epub 1999/11/26. eng.

[69] West MJ. Design-based stereological methods for counting neurons. Progress in Brain Research. 2002;135:43-51. PubMed PMID: 12143362. Epub 2002/07/30. eng.

[70] Rath D, Niemann H. *In vitro* fertilization of porcine oocytes with fresh and frozen-thawed ejaculated or frozen-thawed epididymal semen obtained from identical boars. Theriogenology. 1997;47(4):785-93. PubMed PMID: 16728028. Epub 1997/03/01. eng.

[71] Bhide PG, Day M, Sapp E, Schwarz C, Sheth A, Kim J, et al. Expression of normal and mutant huntingtin in the developing brain. The Journal of Neuroscience : The Official Journal of the Society for Neuroscience. 1996;16(17):5523-35. PubMed PMID: 8757264. Epub 1996/09/01. eng.

[72] DiFiglia M, Sapp E, Chase KO, Davies SW, Bates GP, Vonsattel JP, et al. Aggregation of huntingtin in neuronal

intranuclear inclusions and dystrophic neurites in brain. Science. 199726;277(5334):1990-3. PubMed PMID: 9302293. Epub 1997/09/26. eng.

[73] Ouimet CC, Greengard P. Distribution of DARPP-32 in the basal ganglia: An electron microscopic study. Journal of Neurocytology. 1990;19(1):39-52. PubMed PMID: 2191086. Epub 1990/02/01. eng.

[74] van Dellen A, Welch J, Dixon RM, Cordery P, York D, Styles P, et al. N-Acetylaspartate and DARPP-32 levels decrease in the corpus striatum of Huntington's disease mice. Neuroreport. 2000;11(17):3751-7. PubMed PMID: 11117485. Epub 2000/12/16. eng.

[75] Tippett LJ, Waldvogel HJ, Thomas SJ, Hogg VM, van Roon-Mom W, Synek BJ, et al. Striosomes and mood dysfunction in Huntington's disease. Brain : A Journal of Neurology. 2007;130(Pt 1):206-21. PubMed PMID: 17040921.

[76] Crittenden JR, Graybiel AM. Basal Ganglia disorders associated with imbalances in the striatal striosome and matrix compartments. Frontiers in Neuroanatomy. 2011;5:59. PubMed PMID: 21941467. Pubmed Central PMCID: 3171104.

[77] Keereman V, Fierens Y, Broux T, De Deene Y, Lonneux M, Vandenberghe S. MRI-based attenuation correction for PET/MRI using ultrashort echo time sequences. J Nucl Med. 2010;51(5):812-8. PubMed PMID: 20439508. Epub 2010/05/05. eng.

[78] Gieling ET, Nordquist RE, van der Staay FJ. Assessing learning and memory in pigs. Anim Cogn. 2011;14(2):151-73. PubMed PMID: 21203792. Pubmed Central PMCID: 3040303. Epub 2011/01/05. eng.

[79] Gieling ET, Schuurman T, Nordquist RE, van der Staay FJ. The pig as a model animal for studying cognition and neurobehavioral disorders. Current Topics in Behavioral Neurosciences. 2011;7:359-83. PubMed PMID: 21287323. Epub 2011/02/03. eng.

[80] Wheeler VC, Persichetti F, McNeil SM, Mysore JS, Mysore SS, MacDonald ME, et al. Factors associated with HD CAG repeat instability in Huntington disease. Journal of Medical Genetics. 2007;44(11):695-701. PubMed PMID: 17660463. Epub 2007/07/31. eng.

[81] Lai L, Prather RS. Creating genetically modified pigs by using nuclear transfer. Reproductive Biology and Endocrinology : RB&E. 2003;1:82. PubMed PMID: 14613542. Pubmed Central PMCID: 280726. Epub 2003/11/14. eng.

[82] Polejaeva IA, Chen SH, Vaught TD, Page RL, Mullins J, Ball S, et al. Cloned pigs produced by nuclear transfer from adult somatic cells. Nature. 2000;407(6800):86-90. PubMed PMID: 10993078. Epub 2000/09/19. eng.

[83] Park F. Lentiviral vectors: Are they the future of animal transgenesis? Physiol Genomics. 2007;31(2):159-73. PubMed PMID: 17684037. Epub 2007/08/09. eng.

[84] Trottier Y, Devys D, Imbert G, Saudou F, An I, Lutz Y, et al. Cellular localization of the Huntington's disease protein and discrimination of the normal and mutated form. Nature Genetics. 1995;10(1):104-10. PubMed PMID: 7647777. Epub 1995/05/01. eng.

[85] Wood JD, MacMillan JC, Harper PS, Lowenstein PR, Jones AL. Partial characterisation of murine huntingtin and apparent variations in the subcellular localisation of huntingtin in human, mouse and rat brain. Human Molecular Genetics. 1996;5(4):481-7. PubMed PMID: 8845840. Epub 1996/04/01. eng.

[86] Walaas SI, Greengard P. DARPP-32, a dopamine- and adenosine 3′:5′-monophosphate-regulated phosphoprotein enriched in dopamine-innervated brain regions. I. Regional and cellular distribution in the rat brain. The Journal of Neuroscience : The Official Journal of the Society for Neuroscience. 1984;4(1):84-98. PubMed PMID: 6319627. Epub 1984/01/01. eng.

[87] Hemmings HC, Jr., Greengard P, Tung HY, Cohen P. DARPP-32, a dopamine-regulated neuronal phosphoprotein, is a potent inhibitor of protein phosphatase-1. Nature. 1984;310(5977):503-5. PubMed PMID: 6087160. Epub 1984/08/09. eng.

[88] Bibb JA, Yan Z, Svenningsson P, Snyder GL, Pieribone VA, Horiuchi A, et al. Severe deficiencies in dopamine signaling in presymptomatic Huntington's disease mice. Proceedings of the National Academy of Sciences of the United States of America. 2000;97(12):6809-14. PubMed PMID: 10829080. Pubmed Central PMCID: 18747. Epub 2000/06/01. eng.

[89] Hackam AS, Singaraja R, Wellington CL, Metzler M, McCutcheon K, Zhang T, et al. The influence of huntingtin protein size on nuclear localization and cellular toxicity. The Journal of Cell Biology. 1998;141(5):1097-105. PubMed PMID: 9606203. Pubmed Central PMCID: 2137174. Epub 1998/06/12. eng.

[90] Chen S, Berthelier V, Hamilton JB, O'Nuallain B, Wetzel R. Amyloid-like features of polyglutamine aggregates and their assembly kinetics. Biochemistry. 2002;41(23):7391-9. PubMed PMID: 12044172. Epub 2002/06/05. eng.

[91] Li SH, Li XJ. Aggregation of N-terminal huntingtin is dependent on the length of its glutamine repeats. Human Molecular Genetics. 1998;7(5):777-82. PubMed PMID: 9536080. Epub 1998/05/23. eng.

[92] Gray M, Shirasaki DI, Cepeda C, Andre VM, Wilburn B, Lu XH, et al. Full-length human mutant huntingtin with a stable polyglutamine repeat can elicit progressive and selective neuropathogenesis in BACHD mice. The Journal of Neuroscience : The Official Journal of the Society for Neuroscience. 2008;28(24):6182-95. PubMed PMID: 18550760. Pubmed Central PMCID: 2630800. Epub 2008/06/14. eng.

[93] Pouladi MA, Stanek LM, Xie Y, Franciosi S, Southwell AL, Deng Y, et al. Marked differences in neurochemistry and aggregates despite similar behavioural and neuropathological features of Huntington disease in the full-length BACHD and YAC128 mice. Human Molecular Genetics. 2012;21(10):2219-32. PubMed PMID: 22328089.

[94] Miller J, Arrasate M, Brooks E, Libeu CP, Legleiter J, Hatters D, et al. Identifying polyglutamine protein species *in situ* that best predict neurodegeneration. Nature Chemical Biology. 2011;7(12):925-34. PubMed PMID: 22037470. Pubmed Central PMCID: 3271120. Epub 2011/11/01. eng.

[95] Van Raamsdonk JM, Murphy Z, Selva DM, Hamidizadeh R, Pearson J, Petersen A, et al. Testicular degeneration in Huntington disease. Neurobiology of Disease. 2007;26(3):512-20. PubMed PMID: 17433700. Epub 2007/04/17. eng.